OLD DOMINION UNIVERSITY RESEARCH FOUNDATION

SCHOOL OF ENGINEERING
OLD DOMINION UNIVERSITY
NORFOLK, VIRGINIA

ACCURATE SPECTRAL MODELING FOR INFRARED RADIATION

By

S. N. Tiwari

and

S. K. Gupta

Progress Report

Prepared for the
National Aeronautics and Space Administration
Langley Research Center
Hampton, Virginia 23665

Under
Research Grant NSG 1282
November 1976-January 1977
Dr. Henry G. Reichle, Technical Monitor
Atmospheric Environmental Sciences Division

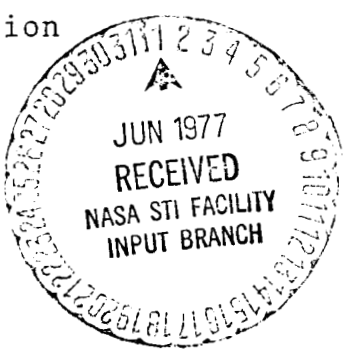

April 1977

SCHOOL OF ENGINEERING
OLD DOMINION UNIVERSITY
NORFOLK, VIRGINIA

Technical Report

ACCURATE SPECTRAL MODELING FOR INFRARED RADIATION

By

S. N. Tiwari

and

S. K. Gupta

Progress Report

Prepared for the

National Aeronautics and Space Administration
Langley Research Center
Hampton, Virginia 23665

Under

Research Grant NSG 1282
November 1976-January 1977
Dr. Henry G. Reichle, Technical Monitor
Atmospheric Environmental Sciences Division

Submitted by the

Old Dominion University Research Foundation
Norfolk, Virginia 23508

April 1977

FOREWORD

This report constitutes a part of the work done on the research project entitled "Determination of Atmospheric Pollutants from Infrared Radiation Measurements." The work was supported by the NASA - Langley Research Center (Atmospheric Systems Branch of the Atmospheric Environmental Sciences Division) through Grant NSG 1282. The grant was monitored by Dr. Henry G. Reichle, Jr.

TABLE OF CONTENTS

LIST OF FIGURES

LIST OF TABLES

ACCURATE SPECTRAL MODELING FOR INFRARED RADIATION

S. N. Tiwari* and S. K. Gupta†

SUMMARY

Direct line-by-line integration and quasi-random band model techniques are employed to calculate the spectral transmittance and total absorptance of 4.7μ CO, 4.3μ CO_2, 15μ CO_2, and 5.35μ NO bands. Results are obtained for different pressures, temperatures and path lengths. These are compared with available theoretical and experimental investigations. For specific pressure, temperature, and path length conditions, experimental results for total absorptance are also available in the literature for the gases under present investigation. For exactly the same conditions, total absorptance was also calculated by employing the line-by-line and quasi-random band models and the continuous correlations of Tien and Lowder, Cess and Tiwari and Felske and Tien. For each gas, extensive tabulations of results are presented for comparative purposes. In almost all cases, line-by-line results are found to be in excellent agreement with the experimental values. The range of validity of other models and correlations are discussed.

*Professor, †Research Associate, School of Engineering, Old Dominion University, Norfolk, Virginia 23508.

LIST OF SYMBOLS

A = total band absorptance, cm^{-1}

A_o = band width parameter (correlation quantity), cm^{-1}

$\bar{A}(u,\beta)$ = dimensionless band absorptance, $\bar{A} = A/A_o$

d = average line spacing, cm^{-1}

p or P = gas pressure, atm

S, $S(T)$ = total band intensity, atm^{-1}- cm^{-2}

t = line structure parameter, $t = \beta/2$

T = temperature, °K

u = dimensionless coordinate, $u = Spy/A_o$

y = physical coordinate

α_ω = spectral band coefficient

β = line structure parameter, $\beta = 2t$

γ_L = rotationally averaged line half-width, cm^{-1}

κ_ω = volumetric spectral absorption coefficient, $(atm\text{-}cm)^{-1}$

τ_ω = spectral transmittance

ω = wave number, cm^{-1}

ω_o = wave number at the band center, cm^{-1}

1. INTRODUCTION

In radiative transfer analyses, involving infrared active molecules, it often becomes essential to employ meaningful, computationally fast and accurate spectral models for absorption by the absorbing-emitting molecules. The most accurate theoretical procedure to compute the absorptance of a vibration-rotation band is probably the direct integration (line-by-line) method. This employees an appropriate line profile (Lorentz, Doppler, Voigt, etc.) for the given pressure and temperature conditions, and calculates absorption at a large number of frequencies within the spectral range of interest. Although it requires the knowledge of individual line parameters and involves lengthy calculations, the line-by-line method is quite reliable.

Several "narrow" and "wide" band models and band model correlations for infrared spectral absorption have been proposed in the literature [1-17]*. Narrow band models (viz., Elsasser, statistical, random-Elsasser, and quasi-random) can be used for spectral absorptance computations when high resolution is not required. Although the use of these models results in considerable reduction of computational time, the results, in general, have lower degree of accuracy than those obtained by the line-by-line method [19-21]. The quasi-random band model, introduced by Wyatt et al. [6], is the best among the narrow band models to represent the absorption of a vibration-rotation band accurately. In many engineering applications involving a single absorbing-emitting gas, quite often it is possible to make use of the so-called wide band models [8-13]. The relations for total band absorptance of a wide band are obtained from the absorptance formulations of the narrow bands by employing an exponential variation of the line intensities. As such, these models are called the exponential wide band models. In addition, several correlations for the total band

*Numbers in brackets indicate references.

absorptance of a wide band are available in the literature [8-17]. For some gases, these correlations satisfactorily represent the band absorptance over certain ranges of physical conditions. Results of various wide band models and correlations were compared in [16-18]. It was noted that different band models and correlations predict the total absorptance of a band with varying degree of accuracy. Recently, attempts have also been made to express band absorptance relations directly in terms of the basic spectroscopic variables [22-24]. All these results indicate that while a particular formulation (band model relation or correlation) may be applicable to linear molecules, it may give erroneous results when applied to asymmetric or spherical top molecules.

The purpose of this study is to calculate the spectral transmittance and total band absorptance of 4.7μ CO, 4.3μ CO_2, 15μ CO_2, and 5.35μ NO bands by employing the direct line-by-line integration and quasi-random band model techniques. Specific results are obtained for the temperature, pressure, and path length conditions for which experimental measurements are available. Various theoretical and experimental results are compared in order to establish the validity of a particular formulation to specific applications. General results for total band absorptance are obtained for different temperatures, pressures, and path lengths, and these are compared with the results of various correlations.

2. GOVERNING EQUATIONS

For a homogeneous path, the spectral absorptance, α_ω, at wavenumber ω is defined as

$$\alpha_\omega = 1 - \tau_\omega = 1 - \exp(-\kappa_\omega X) \tag{2.1}$$

where τ_ω represents the spectral transmittance, κ_ω is the volumetric absorption coefficient, and $X = py$ is the pressure path length. The total (integrated) band absorptance, over a spectral interval $\Delta\omega$, is given by

$$A = \int_{\Delta\omega} \alpha_\omega \, d\omega = \int_{\Delta\omega} [1-\exp(-\kappa_\omega X)] \, d\omega \tag{2.2}$$

The total band absorptance of a wide band, in turn, is given by

$$A = \int_{-\infty}^{\infty} [1-\exp(-\kappa_\omega X)] \, d(\omega-\omega_o) \tag{2.3}$$

where the limits of integration are over the entire band pass and ω_o is the wavenumber at the center of the wide band.

For the present study, it is convenient to define the integrated band absorptance in a nondimensional form as

$$\bar{A} = A/A_o \tag{2.4}$$

where A_o is the band width parameter [9-12]. Also, the optical path length is defined as

$$u = S \, X/A_o = S \, py/A_o \tag{2.5}$$

where S represents the integrated band intensity.

Various theoretical formulations of narrow and wide band models are reviewed in [11-13,16,17]. The wide band correlations, whose results are compared in this study, are discussed here briefly. A three-piece correlation was introduced first by Edwards and Menard [8,9]. The first continuous correlation was proposed by Tien and Lowder [10,11], and this is of the form

$$\bar{A}(u,\beta) = \ell n(u\, f(t)\{(u + 2)/[u + 2f(t)]\} + 1) \tag{2.6}$$

where

$$f(t) = 2.94[1-\exp(-2.60\ t)]\ ,\ t = \beta/2\ ,\ \beta = 2\pi\gamma_L/d$$

A continuous correlation introduced by Cess and Tiwari is given by

$$\bar{A}(u,\beta) = 2\ \ell n(1 + u/\{2 + [u(c + \pi/2\beta)]^{1/2}\}) \tag{2.7}$$

Different values for constant c in Eq. (2.7) are suggested in [16,17]. If it is desired to use only one value of c for all β and path lengths, the value of $c = 0.1$ is recommended. Felske and Tien [14] have proposed a continuous correlation of the form

$$\bar{A}(u,\beta) = 2\ E_1(t\rho_u) + E_1(\rho_u/2) - E_1[(\rho_u/2)(1 + 2t)]$$

$$+ \ell n[(t\ \rho_u)^2/(1 + 2t)] + 2\gamma \tag{2.8}$$

where

$$\rho_u = \{(t/u)[1 + (t/u)]\}^{-1/2}\ ,\ \gamma = 0.5772156$$

Since this correlation involves exponential integral functions, it requires relatively longer computational time when used in radiative transfer analyses [18]. Based on the theoretical formulation of Edwards and Menard [8,9], Green and Tien have proposed a piecewise correlation for NO in [25]. Results of these correlations are compared with other theoretical and experimental results in sections 4 and 5.

As discussed in [7,12,17], band absorptance relations possess several limiting forms. At sufficiently low pressure path lengths (i.e., for $u \ll 1$), the nondimensional total band absorptance is given by the linear limit as

$$\bar{A} = u \tag{2.9}$$

At large path lengths (i.e., for $u >> 1$), the total band absorptance is given by a logarithmic asymptote as

$$\bar{A} = \ell n\, u \tag{2.10}$$

In the large path length limit most of the correlations reduce to [17]

$$\bar{A} = \ell n\, u + \gamma \tag{2.11}$$

Since $\gamma = 0.5772$, Eq. (2.11) usually is expressed as

$$\bar{A} = \ell n\, u + 1 \tag{2.12}$$

For sufficiently large values of u Eqs. (2.11) and (2.12) reduce to Eq. (2.10). In this study, Eq. (2.12) is employed for the band absorptance in the large path length limit.

If the band absorptance results obtained by employing the line-by-line model can be treated as exact results, then errors in using results of any other formulation can be expressed by the relation

$$\% = PD = [(\bar{A} - \bar{A}_E)/\bar{A}_E] \times 100 \tag{2.13}$$

where $\bar{A}_E = A_E/A_o$ and A_E represents the line-by-line absorptance. Results for different gases, as obtained by using Eq. (2.13) are presented in section 5.

3. COMPUTATIONAL PROCEDURE

The procedure used for computing the spectral transmittance and total band absorptance by employing the line-by-line and quasi-random band models are described in detail in [6,19,26-28]. These are discussed here briefly.

The direct integration (line-by-line) method consists of calculating the absorption coefficient, and then the transmittance, at a large number of frequency locations within the spectral range of interest. Since the absorption coefficient is a fast varying function of the frequency (varying by orders of magnitude over the width of a line), it has to be evaluated at very closely spaced locations. The total absorption coefficient at any frequency location is made up of contributions from a large number of lines in the vicinity of that frequency. This method yields results with a high degree of accuracy. However, the evaluation of total absorptance of a band with a large number of lines requires a considerably long computational time. Drayson [26] and Kunde and Maguire [28] have proposed a scheme for the evaluation of transmittance using this method. The procedure and computer program developed for this work is a modification of the methods discussed in the above references. It makes use of the Lorentz line profile for absorption coefficient and is relatively simple and efficient. The entire procedure is discussed in detail in [19]. The line parameters needed in the calculation are obtained from McClatchey et al. [29].

The quasi-random band model was introduced by Wyatt, Stull, and Plass [6]. A revised version of this model was applied by Kunde [27] to several planetary atmospheric applications and satisfactory results were obtained. The procedure and computer program used in the present work differs from that used in [27]. It is a highly simplified numerical integration scheme which requires considerably less computational time. The procedure is discussed in detail in [19].

4. SPECIFIC COMPARISONS OF SPECTRAL TRANSMITTANCE AND TOTAL BAND ABSORPTANCE

For the gases under consideration, experimental band absorptance results are available in the literature [25,30,31]. For the 4.7μ CO fundamental band experimental results were obtained from Burch et al. [30] and Abu-Romia and Tien [31]. For the 15μ and 4.3μ CO_2 bands experimental results were obtained from Burch et al. [30] and for the 5.35μ NO band the results were obtained from Green and Tien [25]. By employing the line-by-line (LBL) and quasi-random band (QRB) models, specific results were obtained for exactly the same temperature, pressure, and path length conditions for which experimental measurements were available. For the same conditions, results were also obtained by employing the continuous correlations of Tien and Lowder [10,11], Cess and Tiwari [10,16], and Felske and Tien [14]. The correlation quantities required in the calculation were obtained from [9-11]. Various theoretical and experimental band absorptance results are compared in this section.

For the 4.7μ CO fundamental band, the spectral range considered is between 1975-2265 cm^{-1}. In this range, there are 254 spectral lines. The line parameters for this band were obtained from McClatchey et al. [29]. By employing the LBL and QRB models, spectral transmittance results were obtained for this band in the spectral range 2070-2220 cm^{-1} for conditions $T = 300°K$, $P_e = 51$ mm Hg, and $X = 22.8$ cm-atm [20]. A comparison of these with experimental results (see Fig. 4.1) indicates that the LBL results are in good agreement with the experimental values while QRB results exhibit appreciable differences (particularly in the P and R branches of the band). The integrated intensity of the band was found to be 261 cm^{-2} atm^{-1} at $T = 300°K$. By employing the LBL and QRB models and the continuous correlations, total absorptance results were

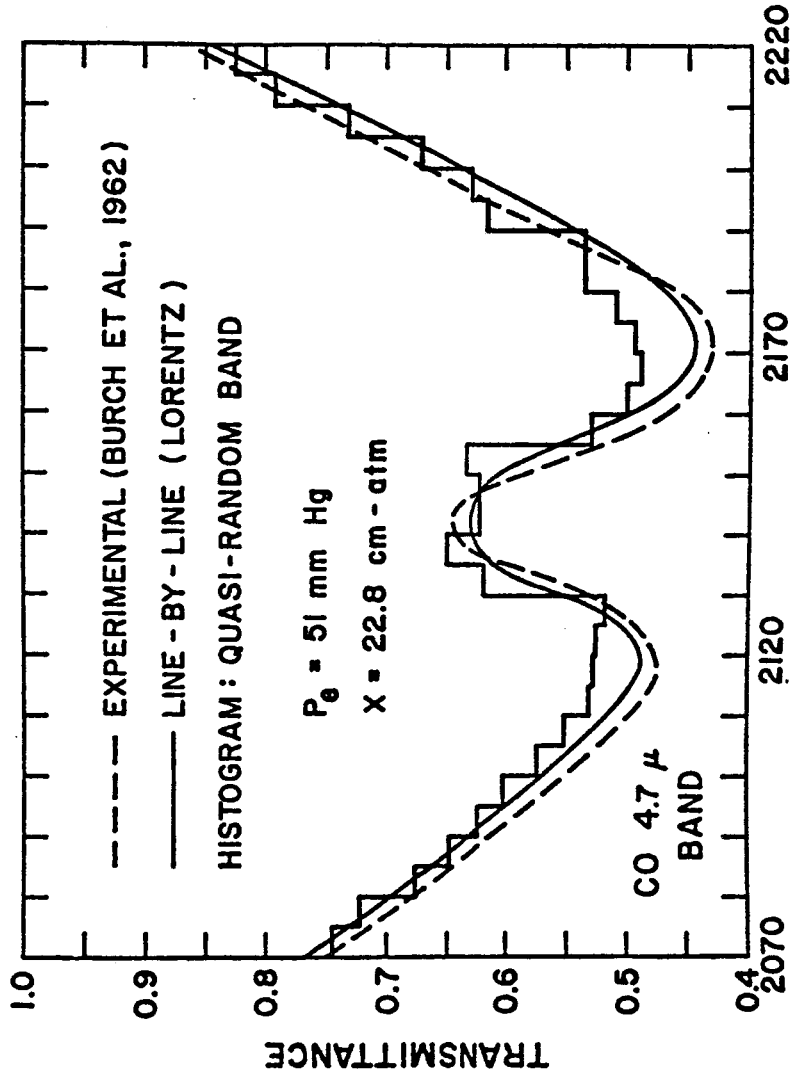

Fig. 4.1 Comparison of transmittances of the CO fundamental band at T = 300°K.

obtained for this band at T = 300°K. The results are presented in Tables 4.1 and 4.2 along with other theoretical and experimental results. The comparison shows that the LBL and QRB results are in good agreement with the experimental results (LBL being slightly better than QRB). Among other theoretical results, the results of HHG (Hashemi, Hsieh and Greif [24] provides the best agreement with the experimental and LBL results. Among the results of the correlations, it can be seen that, for the very low pressures, the Tien and Lowder's correlation yields higher values of absorptance and Cess and Tiwari and Felske and Tien's correlations show better agreement. For medium and high pressures, however, Tien and Lowder's correlation yields better agreement while Cess and Tiwari and Felske and Tien's correlations yield much lower values. One may conclude, therefore, that use of the Tien and Lowder's correlation is justified in radiative transfer analyses involving CO at relatively high pressures.

The line parameters for the 15μ CO_2 fundamental band were obtained from [29]. There are more than 7,200 lines in the spectral range (550-800 cm^{-1}) of this band. Spectral transmittances of this band were calculated by using the LBL and QRB models for T = 300°K, P_e = 1100 mm Hg, and X = 1.55 cm-atm [20]. These are illustrated in Fig. 4.2 along with the experimental results. The agreement between the three results is seen to be excellent. The integrated intensity of the band was found to be approximately 252 cm^{-2} atm^{-1} at T = 300°K. For this band, total band absorptance results were calculated by employing the LBL and QRB models and the continuous correlations at T = 300°K. The QRB results for this band are given also by Kunde [27] and Young [32]. The results are presented in Table 4.3 for six illustrative cases. Because of the large computer time required for the LBL computation, only six sample cases were considered. The time required by the QRB model was remarkably low (approximately a factor of 14 lower than the LBL computation) for this band. An

Table 4.1 Comparison of absorptance results for the 4.7μ fundamental band of carbon monoxide at T = 300 °K (experimental data of Burch et al. [30]); HHG = Hashemi, A., Hseih, T. C., and Greif, R. [24] LBL = line-by-line, QRB = quasi-random band.

Eff.Pr. [24] P_e (atm)	Eff.Pr. [30] P_e (atm)	Pr.Path Length [30] P_a y (atm-cm)	Opt. Path u	Absorptance Results, A (cm^{-1})							
				Exp. [30]	Theoretical				Correlation		
					HHG [24]	Edwards & Menard [8-9]	Present LBL	Present QRB	Tien & Lowder [10]	Cess & Tiwari [12,16]	Felske & Tien [14]
0.0329	0.0329	0.0110	0.0686	0.84	0.92	1.3	0.737	0.974	1.0132	0.8091	0.8318
0.0345	0.0345	1.3752	8.5771	14.2	12.6	17.0	12.86	13.00	7.9414	11.9875	11.3233
0.337	0.3368	0.0028	0.0175	0.64	0.64	0.68	0.650	0.678	0.6402	0.4906	0.5789
0.317	0.3171	0.4366	2.7231	20.5	21.4	22.9	20.55	19.88	22.6158	16.6929	17.1523
0.312	0.3118	15.175	94.647	110.0	108.0	119.7	110.24	104.45	113.3707	75.2403	83.3990
3.97	3.974	0.0028	0.0175	0.69	0.68	0.68	0.723	0.726	0.6635	0.5925	0.6543
3.91	3.908	0.0753	0.4696	16.3	16.5	17.4	16.50	16.11	15.6790	10.2476	12.7278
3.91	3.908	1.3752	8.5771	102.6	113.5	97.5	101.95	94.49	100.0165	58.6714	69.7050
3.91	3.908	15.175	94.647	183.4	187.6	188.6	185.31	184.43	193.0015	133.2973	155.5740
1.01	1.015	47.421	295.765	184.6	183.4	197.7	187.05	186.93	196.6126	138.9117	160.9919

Table 4.2a Comparison of absorptance results for the 4.7μ fundamental band of carbon monoxide at 300°K (experimental data of Abu-Romia and Tien [31]); HHG = Hashemi, A., Hseih, T. C. and Greif, R. [24], LBL = line-by-line, QRB = quasi-random band.

Eff.Pr. P_e (atm)	Pr.Path Length P_a y (atm-cm)	Opt. Path* u	Absorptance Results, A (cm^{-1})							
			Exp. [31]	Theoretical				Correlation		
				HHG [24]	Edwards & Menard [8-9]	Present LBL	Present QRB	Tien & Lowder [10]	Cess & Tiwari [12,16]	Felske & Tien [14]
0.51	0.5	2.95	22.0	27.3	27.8	27.43	26.25	31.16	20.50	21.59
1.02	1.0	5.90	48.5	54.6	52.2	53.24	50.03	60.26	36.06	39.63
2.04	2.0	11.81	90.0	100.5	93.8	96.49	89.67	98.79	58.91	63.83
0.255	1.25	7.38	30.2	31.5	34.5	32.18	31.09	33.82	25.36	25.88
1.02	5.0	29.50	112.0	109.3	110.0	109.68	103.05	111.7	70.62	79.83
3.06	15.0	88.60	193.5	181.2	180.8	180.86	179.33	184.5	126.02	147.2
1.02	10.0	59.10	148.0	136.8	136.4	138.23	131.63	136.7	89.29	102.3
1.02	20.0	118.10	169.0	160.5	162.8	163.35	159.18	162.3	109.7	126.9
2.04	40.0	236.20	210.0	193.0	208.0	196.57	197.42	210.4	150.0	173.7
3.06	60.0	354.30	226.0	207.5	233.6	210.80	212.45	237.3	174.5	200.0

*u-values were obtained from [24].

Table 4.2b Comparison of absorptance results for the 4.7μ fundamental band of carbon monoxide at 300°K (experimental data of Abu-Romia and Tien [31]); HHG = Hashemi, A., Hseih, T. C. and Greif, R. [24], LBL = line-by-line, QRB = quasi-random band.

Eff.Pr. P_e (atm)	Pr.Path Length P_a y (atm-cm)	Opt. Path* u	Absorptance Results, A (cm^{-1})							
			Exp. [31]	Theoretical				Correlation		
				HHG [24]	Edwards & Menard [8-9]	Present LBL	Present QRB	Tien & Lowder [10]	Cess & Tiwari [12,16]	Felske & Tien [14]
0.51	0.5	3.119	22.0	27.3	27.8	27.43	27.43	32.08	21.11	22.23
1.02	1.0	6.237	48.5	54.6	52.2	53.24	50.03	61.81	37.03	40.72
2.04	2.0	12.474	90.0	100.5	93.8	96.49	89.67	100.74	60.26	69.43
0.255	1.25	7.796	30.2	31.5	34.5	32.18	31.09	34.85	26.03	26.57
1.02	5.0	31.185	112.0	109.3	110.0	109.68	103.05	113.66	72.03	81.53
3.06	15.0	93.555	193.5	181.2	180.8	180.86	179.33	186.56	127.86	149.31
1.02	10.0	62.370	148.0	136.8	136.4	138.23	131.63	138.65	90.82	104.16
1.02	20.0	124.740	169.0	160.5	162.8	163.35	159.18	164.32	111.41	128.86
2.04	40.0	249.480	210.0	193.0	208.0	196.57	197.42	212.51	151.92	175.80
3.06	60.0	374.220	226.0	207.5	233.6	210.80	212.45	239.43	176.48	202.12

*u-values were calculated by using the relation $u = SPy/A_o$.

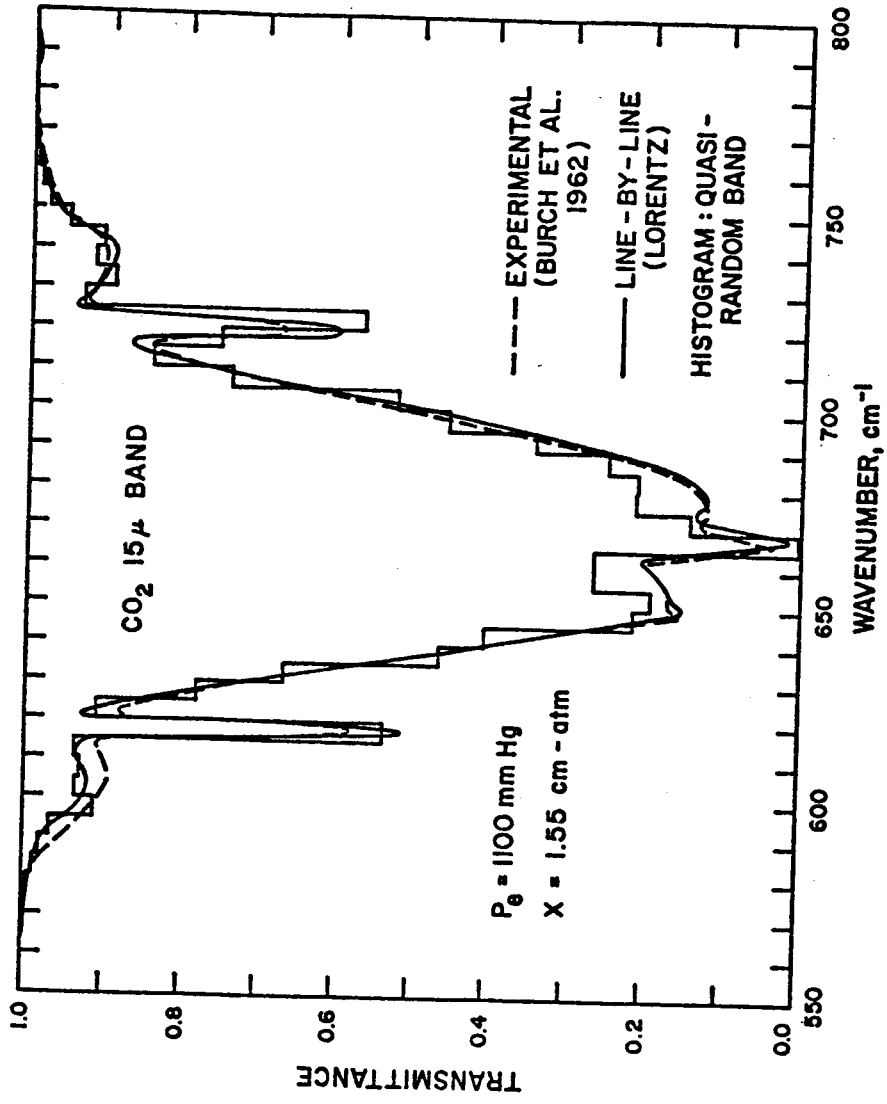

Fig. 4.2 Comparison of transmittances of the 15μ CO_2 band at T = 300°K.

4.3 Comparison of absorptance results for the 15μ fundamental band of carbon dioxide at T = 300 °K (experimental data of Burch et al. [30] and Kunde [27]; LBL = line-by-line; QRB = quasi-random band.

Path Length	Eff. Pr. [30]	Eff. Pr. [27]	Pr.Path Length [27,30]	Pr.Path Length [30]	Opt. Path	Absorptance Results, A (cm^{-1})							
						Exp. [30]	Theoretical				Correlation		
							Young [33]	Kunde [27]	Present	Present	Tien & Lowder [10]	Cess & Tiwari [12,16]	Felske & Tien [14]
y (cm)	P_e (mm Hg)	P_e (atm)	P_a y (atm-cm)	P_a y (atm-cm)	u		QRB	QRB	LBL	QRB			
400	15.6	0.0205	5.73	5.7474	87.378	34.6	43.3	34.4	35.44	37.49	17.36	16.08	15.72
400	63.6	0.0837	5.73	5.7474	87.378	54.7	67.3	53.6	56.42	57.54	39.11	27.81	28.90
400	304.0	0.4000	5.73	5.7474	87.378	81.9	94.0	79.2	83.23	83.47	69.93	46.25	51.68
400	767.0	1.0092	5.73	5.7474	87.378	95.3	103.9	93.2	86.39	96.91	88.41	58.89	67.85
1,600	3.77	0.0050	5.56	5.5558	84.465	21.7	26.7	20.1	19.88	24.7	5.48	8.57	8.02
1,600	6.24	0.0083	9.20	9.1958	139.804	32.6	39.3	30.4	30.81	34.18	12.58	13.43	12.91

inspection of the Table shows that the LBL results agree very well with the experimental results. The present QRB results are higher than the experimental values for very low pressures, but they agree well at moderate and high pressures. Young's results are consistently higher while Kunde's results agree very well. Looking at the results of continuous correlations, it is noted that Tien and Lowder's results are very low at lower pressures but compare better at the higher pressures. The results of Cess and Tiwari and Felske and Tien's correlation are consistently lower for all cases considered.

The line parameters for the 4.3μ CO_2 band were obtained also from [29]. There are approximately 5,565 lines in the spectral range (2220-2420 cm^{-1}) of this band. Experimental and theoretical transmittance results for this band are compared in Fig. 4.3 for T = 300, P_e = 274 mm Hg, and X = 0.338 cm-atm [20]. The agreement between the experimental and LBL results is seen to be excellent. The QRB results, however, exhibit a slightly lower absorption. The integrated band intensity of this band was found to be approximately 2867 cm^{-2} atm^{-1} at T = 300°K. By employing the LBL and QRB models and the continuous correlations, total band absorptance results were obtained for T = 300°K. For this band also, only six sample cases were considered because of the large time requirement of the LBL computations. No other theoretical results for this band seem to be available in the literature. The results of present computations are presented in Table 4.4 along with the experimental values of Burch et al. [30]. The table indicates excellent agreement between the experimental and present LBL results. The QRB results also are seen to compare very well. Among the results of correlations, Tien and Lowder's results are seen to be lower for low pressures but they compare better at high pressures. Cess and Tiwari and Felske and Tien's results are again found to be consistently low.

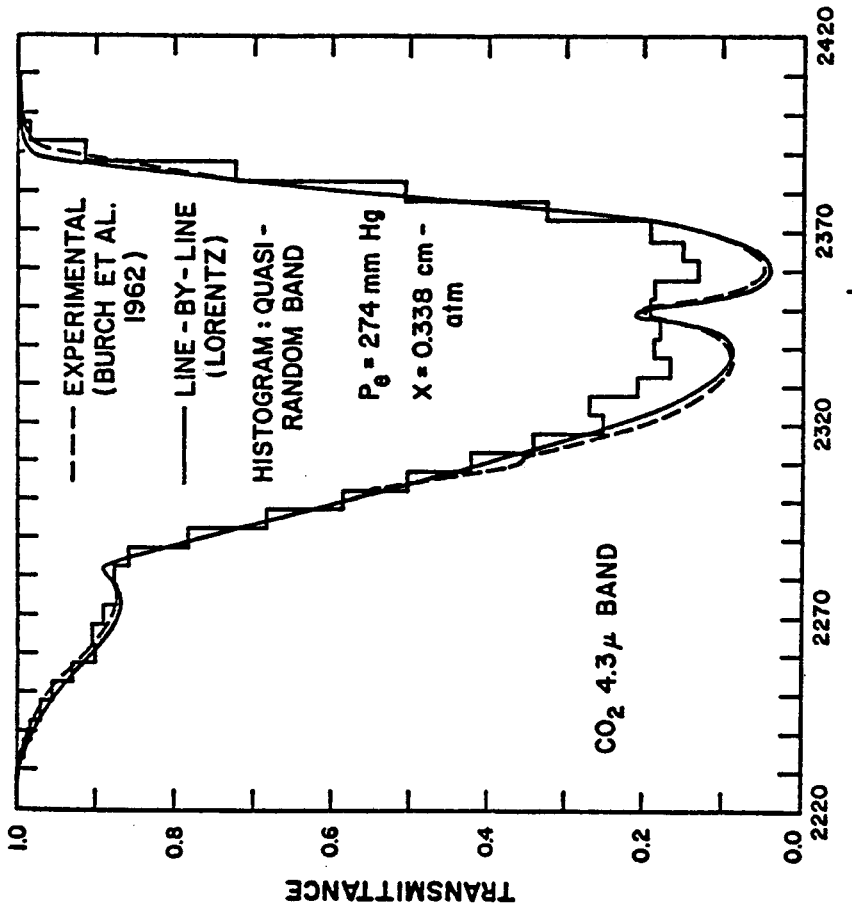

Fig. 4.3 Comparison of transmittances of the 4.3μ CO_2 band at T = 300°K.

Table 4.4 Comparison of absorptance results for the 4.3μ fundamental band of carbon dioxide of T = 300°K (experimental data of Burch et al. [30]; LBL = line-by-line; QRB = quasi-random band.

Cell Length	Eff.Pr.	Eff.Pr.	Pr.Path Length	Pr.Path Length [30]	Opt. Path	Absorptance Results, A (cm^{-1})					
						Exp. [30]	Theoretical		Correlation		
y (cm)	P_e (mm Hg)	P_e (atm)	P_a y (atm-cm)	P_a y (atm-cm)	u		Present LBL	Present QRB	Tien & Lowder [10]	Cess & Tiwari [12,16]	Felske & Tien [14]
1.55	203	0.2671	0.0108	0.011	1.0663	11.7	12.03	11.75	11.19	6.79	7.43
1.55	812	1.0684	0.0234	0.0235	2.3103	29.1	30.03	27.92	26.40	15.00	17.78
1.55	137	0.1803	0.195	0.1948	19.253	48.3	47.80	45.00	40.14	28.83	27.92
12.8	810	1.0658	0.043	0.044	4.2455	41.2	41.90	38.71	36.84	20.94	24.62
12.8	24	0.0318	0.169	0.17	16.686	23.3	22.94	22.50	14.62	12.95	12.80
12.8	218	0.2868	2.55	2.5493	251.767	107.0	106.96	105.27	96.01	66.95	77.54

For the 5.35μ NO band, the line parameters were obtained from the compilation of Goldman and Schmidt [33]. The spectral range considered for this band is 1750-2000 cm^{-1} where there are approximately 1450 rotational lines. The integrated intensity for this band was found to be 112 cm^{-2} atm^{-1}. Goldman and Schmidt used a value of $S = 122$ cm^{-2} atm^{-1} in the generation of line parameters. This difference can be attributed to the presence of additional lines in the wings of the band beyond the above spectral range. The band correlation parameters were obtained from Green and Tien [25]. The u and β values for this band are listed also in [24]. By employing the LBL and QRB models and the correlations, total band absorptance results were calculated for T = 300°K. These are presented in Table 4.5 along with theoretical results of HHG [24] and theoretical and experimental results of Green and Tien [25]. It is seen that the present LBL results are in excellent agreement with the experimental values. Also, except for a few cases, the present QRB results are within 10 per cent of the experimental results. Among the correlation results, Tien and Lowder's results, although lower, compare best with the experimental values. Cess and Tiwari and Felske and Tien's correlations yield much lower values.

Results presented in this section consistently show that the LBL results are in excellent agreement with the experimental values. In most cases QRB results are better than results of any other theoretical formulation. The results of various correlations agree with varying degree of accuracy depending upon the nature of the gas. As such, one should be very careful in applying a correlation to a particular application.

In order to give an idea of comparative computational time and cost involved in calculating the total band absorptance, let us consoder, for example, the case of 15μ CO_2 band results presented in Table 4.3. All these results were obtained from programs run on the CDC-CYBER 175 machine. The time and cost for computing these results by using the LBL and QRB models are as follows:

Table 4.5 Comparison of absorptance results for the 5.35μ fundamental band of nitric oxide at T = 300 °K (experimental data of Green and Tien [25]; HHG = Hashemi, A., Hseih, T. C., and Greif, R. [24], LBL = line-by-line; QRB = quasi-random band.

Eff. Pr.	Pr. Path Length	Opt. Path*	Absorptance Results, A (cm^{-1})							
			Exp. [25]	Theoretical				Correlation		
P_e (atm)	P_a y (atm-cm)	u		Green & Tien [32]	HHG [24]	Present	Present	Tien & Lowder [10]	Cess & Tiwari [12,16]	Felske & Tien [14]
1.0	0.845	2.69	35.76	36.2	31.0	37.93	45.09	28.91	18.43	19.60
1.0	2.45	7.81	67.37	64.6	53.0	64.33	75.83	48.43	30.78	33.06
2.025	1.71	5.45	64.99	65.6	62.0	69.51	78.24	54.38	32.23	35.87
2.025	4.96	15.80	113.92	111.6	97.0	108.90	119.13	81.66	50.56	57.22
3.05	2.575	8.20	91.44	92.0	88.1	97.09	104.93	72.45	42.99	49.18
3.05	7.47	23.80	142.7	139.9	127.5	136.87	144.21	102.45	64.77	75.03
2.98	9.195	29.29	142.7	148.7	134.0	143.84	151.08	107.96	69.13	80.17
4.075	3.44	10.96	108.15	111.7	109.5	113.64	119.83	85.95	51.75	60.21
4.075	9.97	31.76	157.54	159.6	146.7	153.59	159.47	117.16	75.75	88.42
4.075	12.56	40.01	157.40	169.9	153.2	160.53	166.55	124.01	81.40	95.24

*u-values were obtained from [24].

Model	Time (sec)	C. R. Units	Cost
LBL	550	2244	$58.00
QRB	40	180	$ 7.00

This indicates that the time, computer resource (CR) units and cost in dollars associated with QRB calculations are approximately an order of magnitude lower than for the LBL computations. This will be true for any band which has a large number of (several thousands) lines. For bands which have smaller number of lines, this difference is less dramatic. A single program was used to compute the absorptance for all four bands (4.7μ CO, 15μ CO_2, 4.3μ CO_2, and 5.35μ NO) using all three correlations (Tien and Lowder, Cess and Tiwari, and Felske and Tien). The computer resource units used by this program are, in general, a factor of 5 lower than those used by the QRB program. It will be safe to assume, therefore, that the use of the various correlations results in at least another order of magnitude reduction in computer usage.

5. GENERAL PARAMETRIC COMPARISONS OF TOTAL BAND ABSORPTANCE

General band absorptance results were obtained by employing the LBL and QRB models and the continuous correlations of Tien and Lowder, Cess and Tiwari, and Felske and Tien. The sources of various correlation quantities and line parameters used in the computation are already mentioned in the previous section. For different gases (4.7μ CO, 15μ CO_2, 4.3μ CO_2, and 5.35μ NO), results were obtained for P = 0.01, 0.1, 1.0, and 10 atm and for T = 300°K and 500°K. The results are presented in Tables 5.1 - 5.4 and also are illustrated in Figs. 5.1 - 5.4. For CO fundamental band, results of all formulations are illustrated in Figs. 5.1 for three different pressures. For the sake of clarity, results for CO_2 and NO bands are compared only for the LBL, QRB, and Tien and Lowder's calculations and these are illustrated in Figs. 5.2 - 5.4 for different pressures. If the results for one and ten pressures were very close, then in some figures they are illustrated for P = 1 atm, and in others for P = 10 atm. In a particular application, if one needs to compare all the results for any specific pressure and temperature, then these results can be drawn from the data presented in Tables 5.1 - 5.4.

In order to calculate the per cent error in using a particular formulation, the LBL results are treated as exact results in this section. Per cent errors in total absorptance of various bands were calculated by employing Eq. (2.13). These are illustrated in Figs. 5.5 - 5.8 for T = 300°K and different pressures.

For CO fundamental band results presented in Tables 5.1 and illustrated in Figs. 5.1 and 5.5 show that the QRB values are in excellent agreement with the exact (LBL) results except for very low pressures and small optical paths. It is noted that all three correlations exhibit poor agreement with the exact results at the very low pressure of 0.01 atm. At 0.1 atm, however, Cess and

Tiwari, and Felske and Tien correlations yield better agreement than does the Tien and Lowder correlation. At 1.0 atm, all three correlations yield reasonable agreement, although Tien and Lowder correlation yields higher values than the LBL results while the others yield lower values. At 10 atm, Tien and Lowder correlation yields much better agreement than do the others.

For CO_2 bands, general band absorptance results are presented in Tables 5.2 and 5.3, and are illustrated in Figs. 5.2, 5.3, 5.6 and 5.7. It is noted, in general that the LBL and QRB results are in excellent agreement for $p \geq 1$. Since CO_2 bands contain a relatively large number of lines, the large pressure limit for these bands is achieved at relatively low pressures (at about 2-5 atmospheres, depending on the temperature). Because of the nature of variation of the Lorentz line widths with temperature and pressure, the LBL and QRB results for $p = 1$ and 10 atmospheres are closer at 500°K than at 300°K.

For 15μ CO_2 band, the QRB results are in excellent agreement with the LBL results except for very low pressures and small optical paths (see Tables 5.2 and Figs. 5.2 and 5.6). Of the three correlations, the Tien and Lowder correlation shows fair agreement with the exact results for the entire range of physical conditions. The Cess and Tiwari, and Felske and Tien correlations, on the other hand, yield consistently lower values than the LBL results.

For the 4.3μ CO_2 band also, the QRB results show an excellent agreement with the LBL results (see Tables 5.3, and Figs. 5.3 and 5.7). Among the correlations, Cess and Tiwari, and Felske and Tien correlations exhibit much better agreement with LBL results at lower pressures while Tien and Lowder correlation yields much higher values. At moderate and high pressures, however, Tien and Lowder correlation shows much better agreement while others yield results which are consistently lower.

For the NO fundamental band the QRB results (see Table 5.4, and Figs. 5.4 and 5.8) show poor agreement with the LBL results for 0.01 atm and only fair agreement at 0.1 atm. For 1.0 atm the agreement is good and it is excellent at 10 atm. Tien and Lowder correlation yields poor agreement at lower pressures and fair agreement at medium and high pressures. Cess and Tiwari, and Felske and Tien correlations, on the other hand, yield consistently lower values for the entire range of physical conditions.

Results presented in this section indicate that, except for very low pressures, the QRB results are in general agreement with the LBL results for all bands under investigation. It is also noted that no one correlation can be expected to yield accurate results for all gases under all conditions. Use of the Tien and Lowder correlation is recommended for diatomic gases like CO and NO at moderately high pressures. At low and moderate pressures and for gases like CO_2, use of the Cess and Tiwari or Felske and Tien correlations is recommended.

Table 5.1a Comparison of integrated absorptances for CO fundamental band (T = 300 °K); $\bar{A}_E$ = LBL = line-by-line results (exact), PD = $[(\bar{A}-\bar{A}_E)/\bar{A}_E] \times 100$, QRB = quasi-random band results.

P (atm)	Opt. Path	Integrated Absorptance, $\bar{A} = A/A_o$ (Nondimensional)								
		LBL	QRB		Tien & Lowder		Cess & Tiwari		Felske & Tien	
	u	$\bar{A}_E$	$\bar{A}$	PD	$\bar{A}$	PD	$\bar{A}$	PD	$\bar{A}$	PD
0.01	0.01	0.00256	0.00543	112	0.0078	205	0.0052	103	0.0058	127
	0.1	0.00923	0.01865	102	0.0266	188	0.0252	173	0.0254	175
	1.0	0.04368	0.06154	41	0.0490	12.2	0.0947	117	0.0895	105
	10	0.17987	0.19506	8.5	0.1882	4.6	0.3042	69	0.2859	59
	100	0.58160	0.60158	3.4	1.0172	75	0.8523	47	0.8461	45
	1000	1.78416	1.73142	-3.0	2.9095	63	1.9810	11.0	2.1683	21.5
0.1	0.01	0.00757	0.00885	16.9	0.0096	26.8	0.0073	-3.6	0.0087	14.9
	0.1	0.04209	0.04833	14.8	0.0692	64	0.0453	7.6	0.0500	18.8
	1.0	0.17373	0.17554	1.04	0.2355	35.6	0.2008	15.6	0.2030	16.8
	10	0.58028	0.58258	0.4	0.8169	41	0.6591	13.6	0.6624	14.2
	100	1.78141	1.72112	-3.4	2.4804	39	1.6692	-6.3	1.8043	1.3
	1000	3.97998	3.87159	-2.7	4.6890	17.8	3.2966	-17.2	3.7985	-4.6
1.0	0.01	0.00984	0.00991	0.7	0.0099	0.6	0.0086	-12.6	0.0096	-2.4
	0.1	0.08803	0.08786	-0.2	0.0927	5.3	0.0659	-25	0.0791	-10.1
	1.0	0.48446	0.47057	-2.9	0.6032	24.5	0.3573	-26	0.4003	-17.4
	10	1.66303	1.58071	-5.0	2.0257	21.8	1.2245	-26.4	1.3594	-18.3
	100	3.92855	3.80934	-3.0	4.1443	5.5	2.7822	-29	3.2152	-18.2
	1000	5.26491	5.30060	0.7	6.4257	22	4.7884	-9.1	5.4927	4.3
10	0.01	0.00989	0.00996	0.7	0.0100	1.1	0.0093	-6.0	0.0099	0.1
	0.1	0.09729	0.09764	0.4	0.0978	0.5	0.0788	-19	0.0936	-3.8
	1.0	0.83347	0.81708	-2.0	0.8018	-3.8	0.4974	-40	0.6344	-24
	10	3.34830	3.20311	-4.3	2.9833	-10.9	1.7959	-46	2.1862	-35
	100	5.03703	5.04037	0.1	5.4062	7.3	3.8167	-24	4.4318	-12
	1000	5.72133	5.72637	0.1	7.7268	35	6.0608	5.9	6.7392	17.8

Table 5.1b Comparison of integrated absorptances for CO fundamental band (T = 500 °K); $\bar{A}_E$ = LBL = line-by-line results (exact), PD = $[(\bar{A}-\bar{A}_E)/\bar{A}_E] \times 100$, QRB = quasi-random band results.

P (atm)	Opt. Path	Integrated Absorptance, $\bar{A} = A/A_o$ (Nondimensional)								
		LBL	QRB		Tien & Lowder		Cess & Tiwari		Felske & Tien	
	u	$\bar{A}_E$	$\bar{A}$	PD	$\bar{A}$	PD	$\bar{A}$	PD	$\bar{A}$	PD
0.01	0.01	0.00230	0.00510	122	0.0082	257	0.0055	139	0.0062	170
	0.1	0.00750	0.01660	121	0.0319	325	0.0276	268	0.0281	275
	1.0	0.03516	0.05425	54.3	0.0622	76.9	0.1059	201	0.1008	187
	10	0.15025	0.16728	11.3	0.2365	57.4	0.3407	127	0.3225	115
	100	0.48996	0.51513	5.1	1.1869	142	0.9432	92.5	0.9466	93.2
	1000	1.50596	1.48394	-1.5	3.1517	109	2.1441	42.4	2.3711	57.4
0.1	0.01	0.00732	0.00854	16.7	0.0097	32.5	0.0075	2.5	0.0089	21.6
	0.1	0.03609	0.04320	19.7	0.0743	106	0.0484	34.1	0.0541	49.9
	1.0	0.14631	0.15273	4.4	0.2811	92.1	0.2202	50.5	0.2253	54.0
	10	0.49377	0.50476	2.2	0.9604	94.5	0.7262	47.1	0.7390	49.7
	100	1.50476	1.48069	-1.6	2.7112	80.2	1.8105	20.3	1.9803	31.6
	1000	3.44152	3.34125	-2.9	4.9369	43.5	3.4992	1.7	4.0413	17.4
1.0	0.01	0.00978	0.00986	0.8	0.0099	1.2	0.0088	-10.0	0.0097	-0.8
	0.1	0.08443	0.08480	0.4	0.0940	11.3	0.0683	-19.1	0.0822	-2.6
	1.0	0.42424	0.42122	-0.7	0.6468	52.5	0.3799	-10.5	0.4332	2.1
	10	1.42162	1.37998	-2.9	2.1977	54.6	1.3117	-7.7	1.4771	3.9
	100	3.41601	3.31329	-3.0	4.3609	27.7	2.9431	-13.8	3.4164	0.0
	1000	4.39262	4.38827	-0.1	6.6478	51.3	4.9902	13.6	5.7045	29.9
10	0.01	0.00990	0.00995	0.5	0.0100	1.0	0.0099	0.0	0.0099	0.0
	0.1	0.09705	0.09722	0.2	0,0980	1.0	0.0799	-17.7	0.0945	-2.6
	1.0	0.80778	0.79062	-2.1	0.8112	0.4	0.5107	-36.7	0.6609	-18.2
	10	3.08068	2.94970	-4.3	3.0463	-1.1	1.8547	-39.8	2.2818	-25.9
	100	4.34955	4.34867	0.0	5.4992	26.4	3.9222	-9.8	4.5415	4.4
	1000	4.47254	4.47258	0.0	7.8242	74.9	6.1887	38.4	6.8502	53.2

Table 5.2a Comparison of integrated absorptances for the 15μ CO_2 band (T = 300°K); $\bar{A}_E$ = LBL = line-by-line results (exact), PD = $[(\bar{A}-\bar{A}_E)/\bar{A}_E] \times 100$, QRB = quasi-random band results.

P (atm)	Opt. Path	Integrated Absorptance, $\bar{A} = A/A_o$ (Nondimensional)								
		LBL	QRB		Tien & Lowder		Cess & Tiwari		Felske & Tien	
	u	$\bar{A}_E$	$\bar{A}$	PD	$\bar{A}$	PD	$\bar{A}$	PD	$\bar{A}$	PD
0.01	0.01	0.00721	0.01047	45.0	0.0086	19.3	0.0059	-18.2	0.0068	-5.7
	0.1	0.03652	0.04466	22.3	0.0391	7.1	0.0309	-15.4	0.0318	-12.9
	1.0	0.14612	0.17387	19.0	0.0829	-43.0	0.1212	-17.0	0.1166	-20.2
	10	0.49519	0.57559	16.2	0.3111	-37.0	0.3911	-21.0	0.3738	-24.0
	100	1.46054	1.59837	9.4	1.4155	-3.1	1.0658	-27.0	1.0846	-26.0
	1000	3.48069	3.61350	3.8	3.4548	-0.7	2.3557	-32.0	2.6355	-24.3
0.1	0.01	0.00958	0.00970	1.3	0.0097	1.3	0.0076	-20.6	0.0090	-6.0
	0.1	0.07152	0.07628	3.9	0.0758	6.0	0.0494	-30.9	0.0556	-22.3
	1.0	0.31441	0.34072	8.4	0.2975	-5.4	0.2270	-27.8	0.2332	-25.8
	10	1.14415	1.20139	5.0	1.0114	-11.6	0.7497	-34.0	0.7662	-33.0
	100	3.12546	3.17099	1.5	2.7893	-10.8	1.8592	-40.0	2.0415	-35.0
	1000	5.69650	5.81050	2.0	5.0200	-11.9	3.5679	-37.0	4.1229	-28.0
1.0	0.01	0.00983	0.00997	1.4	0.0099	0.7	0.0087	-11.5	0.0097	-1.3
	0.1	0.08711	0.09288	6.6	0.0933	7.1	0.0670	-23.0	0.0805	-7.6
	1.0	0.54372	0.59109	8.7	0.6227	14.5	0.3672	-32.0	0.4145	-23.7
	10	2.14810	2.10968	-1.8	2.1013	-2.2	1.2624	-41.0	1.4102	-34.0
	100	4.81242	4.84289	0.6	4.2393	-11.9	2.8524	-41.0	3.3032	-31.4
	1000	7.32213	7.28145	-0.6	6.5232	-10.9	4.8766	-33.0	5.5859	-23.7
10	0.01	0.00985	0.00994	0.9	0.0100	1.5	0.0092	-6.6	0.0099	0.5
	0.1	0.09422	0.09579	1.7	0.0977	3.7	0.0783	-16.9	0.0932	-1.1
	1.0	0.70662	0.72521	2.6	0.7962	12.7	0.4906	-31.0	0.6211	-12.1
	10	2.96051	2.94170	-0.6	2.9473	-0.4	1.7662	-40.0	2.1389	-28.0
	100	5.56670	5.64848	1.5	5.3540	-3.8	3.7634	-32.4	4.3750	-21.4
	1000	8.05953	8.04364	-0.2	7.6724	-4.8	5.9961	-25.6	6.6818	-17.1

Table 5.2b Comparison of integrated absorptances for the 15μ CO_2 band (T = 500 °K); $\bar{A}_E$ = LBL = line-by-line results (exact), PD = $[(\bar{A}-\bar{A}_E)/\bar{A}_E] \times 100$, QRB = quasi-random band results.

P (atm)	Opt. Path	Integrated Absorptance, $\bar{A} = A/A_o$ (Nondimensional)								
		LBL	QRB		Tien & Lowder		Cess & Tiwari		Felske & Tien	
	u	$\bar{A}_E$	$\bar{A}$	PD	$\bar{A}$	PD	$\bar{A}$	PD	$\bar{A}$	PD
0.01	0.01	0.00792	0.01609	103	0.0089	12.4	0.0062	-21.7	0.0072	-9.1
	0.1	0.04820	0.07974	65.4	0.0453	-6.0	0.0336	-30.3	0.0350	-27.4
	1.0	0.21458	0.29923	39.4	0.1040	-51.5	0.1348	-37.2	0.1309	-39.0
	10	0.74696	0.94482	26.5	0.3849	-48.5	0.4364	-41.6	0.4206	-43.7
	100	2.06163	2.35931	14.4	1.6133	-21.7	1.1729	-43.1	1.2078	-41.4
	1000	4.32747	4.61635	6.7	3.7015	-14.5	2.5339	-41.4	2.8584	-33.9
0.1	0.01	0.00974	0.00990	1.6	0.0097	-0.4	0.0078	-19.9	0.0091	-6.6
	0.1	0.08027	0.08627	7.5	0.0800	-0.3	0.0524	-34.7	0.0598	-25.5
	1.0	0.43641	0.49339	13.1	0.3484	-20.2	0.2477	-43.2	0.2577	-41.0
	10	1.62277	1.79262	10.5	1.1704	-27.9	0.8226	-49.3	0.8519	-47.5
	100	4.03264	4.27449	6.0	3.0228	-25.0	2.0080	-50.2	2.2294	-44.7
	1000	6.45418	6.66196	3.2	5.2663	-18.4	3.7743	-41.5	4.3649	-32.4
1.0	0.01	0.00989	0.01000	1.1	0.0099	0.1	0.0088	-11.0	0.0098	-0.9
	0.1	0.09112	0.09518	4.5	0.0945	3.7	0.0693	-23.9	0.0835	-8.4
	1.0	0.62061	0.69028	11.2	0.6641	7.0	0.3896	-3712	0.4478	-27.8
	10	2.62495	2.79780	6.6	2.2701	-13.5	1.3495	-48.6	1.5289	-41.8
	100	5.45036	5.58857	2.5	4.4523	-18.3	3.0123	-44.7	3.5019	-35.7
	1000	7.67489	7.75469	1.0	6.7417	-12.1	5.0764	-33.9	5.7935	-24.5
10	0.01	0.00988	0.00995	0.7	0.0100	1.2	0.0093	-5.9	0.0100	1.2
	0.1	0.09473	0.09624	1.6	0.0979	3.3	0.0794	-16.2	0.0941	-0.7
	1.0	0.72878	0.75358	3.4	0.8072	10.8	0.5047	-30.7	0.6489	-11.0
	10	3.24084	3.28814	1.5	3.0192	-6.8	1.8281	-43.6	2.2381	-30.9
	100	6.06941	6.08042	0.2	5.4590	-10.1	3.8745	-36.2	4.4923	-26.0
	1000	8.03103	8.05471	0.3	7.7821	-3.1	6.1308	-23.7	6.8004	-15.3

Table 5.3a Comparison of integrated absorptances for CO_2 4.3μ band (T = 300°K); $\bar{A}_E$ = LBL = line-by-line results (exact), PD = $[(\bar{A}-\bar{A}_E)/\bar{A}_E] \times 100$, QRB = quasi-random band results.

P (atm)	Opt. Path	Integrated Absorptance, $\bar{A} = A/A_o$ (Nondimensional)								
		LBL	QRB		Tien & Lowder		Cess & Tiwari		Felske & Tien	
	u	$\bar{A}_E$	$\bar{A}$	PD	$\bar{A}$	PD	$\bar{A}$	PD	$\bar{A}$	PD
0.01	0.01	0.00620	0.00914	47.0	0.0092	48.0	0.0066	6.5	0.0055	-11.3
	0.1	0.02981	0.03704	24.0	0.0544	82.0	0.0377	26.0	0.0401	34.5
	1.0	0.12012	0.13533	12.7	0.1425	18.6	0.1567	30.0	0.1542	28.4
	10	0.42952	0.45536	6.0	0.5157	20.0	0.5093	18.6	0.4977	15.9
	100	1.36398	1.37231	0.6	1.9162	40.0	1.3407	-1.7	1.4050	3.0
	1000	3.48728	3.35253	-3.9	4.0602	16.4	2.8021	-19.6	3.1926	-8.5
0.1	0.01	0.00950	0.00959	1.0	0.0099	4.2	0.0083	-12.6	0.0095	0.0
	0.1	0.06973	0.06966	-0.1	0.0876	25.6	0.0593	-15.0	0.0697	0.0
	1.0	0.31680	0.31561	-0.4	0.4751	50.0	0.2995	-5.5	0.3220	1.6
	10	1.16636	1.13011	-3.1	1.5749	35.0	1.0083	-13.6	1.0792	-7.5
	100	3.24933	3.06648	-5.6	3.5707	9.9	2.3740	-27.0	2.6963	-17.0
	1000	5.52244	5.47292	-0.9	5.8360	5.7	4.2643	-22.8	4.9229	-10.9
1.0	0.01	0.00994	0.00999	0.5	0.0100	0.6	0.0091	-8.4	0.0099	-0.4
	0.1	0.09499	0.09464	-0.4	0.0969	2.0	0.0754	-21.0	0.0905	-4.7
	1.0	0.67912	0.64769	-4.6	0.7613	12.1	0.4561	-32.8	0.5570	-18.0
	10	2.55122	2.35619	-7.6	2.7390	7.4	1.6189	-36.5	1.9140	-25.0
	100	4.89961	4.79504	-2.1	5.0633	3.3	3.4993	-28.6	4.0822	-16.7
	1000	6.92736	6.85839	-1.0	7.3705	6.4	5.6751	-18.0	6.3861	-7.8
10	0.01	0.00989	0.00996	0.7	0.0100	1.1	0.0094	-5.0	0.0099	0.1
	0.1	0.09752	0.09808	0.6	0.0982	0.7	0.0824	-15.5	0.0963	-1.3
	1.0	0.85205	0.84544	-0.8	0.8244	-3.2	0.5454	-36.0	0.7334	-14.0
	10	3.44692	3.39145	-1.6	3.1404	-8.9	2.0124	-42.0	2.5626	-25.6
	100	5.58567	5.60593	0.4	5.6428	1.0	4.2069	-24.7	4.8188	-13.7
	1000	8.21852	8.26854	0.4	7.9753	-3.0	6.5340	-20.5	7.1321	-13.2

Table 5.3b Comparison of integrated absorptances for the CO_2 4.3μ band (T = 500 °K); $\bar{A}_E$ = LBL = line-by-line results (exact), PD = $[(\bar{A}-\bar{A}_E)/\bar{A}_E] \times 100$, QRB = quasi-random band results.

P (atm)	Opt. Path	Integrated Absorptance, $\bar{A} = A/A_o$ (Nondimensional)								
		LBL	QRB		Tien & Lowder		Cess & Tiwari		Felske & Tien	
	u	$\bar{A}_E$	$\bar{A}$	PD	$\bar{A}$	PD	$\bar{A}$	PD	$\bar{A}$	PD
0.01	0.01	0.00650	0.01260	93.8	0.0094	44.6	0.0069	6.2	0.0081	24.6
	0.1	0.03421	0.05100	49.0	0.0605	76.8	0.0407	19.0	0.0439	28.3
	1.0	0.14808	0.19382	30.9	0.1753	18.4	0.1732	17.0	0.1722	16.3
	10	0.54366	0.64038	17.8	0.6238	14.7	0.5651	3.9	0.5581	2.7
	100	1.65293	1.75561	6.2	2.1351	29.2	1.4654	-11.3	1.5548	-5.9
	1000	3.64266	3.63338	-0.3	4.3089	18.3	2.9942	-17.8	3.4299	-5.8
0.1	0.01	0.00953	0.00972	2.0	0.0099	3.9	0.0084	-11.9	0.0096	0.7
	0.1	0.07278	0.07628	4.8	0.0900	23.7	0.0620	-14.8	0.0737	1.3
	1.0	0.36531	0.37722	3.3	0.5281	44.6	0.3223	-11.8	0.3519	-3.7
	10	1.36334	1.37333	0.7	1.7539	28.6	1.0924	-19.9	1.1863	-13.0
	100	3.42711	3.37961	-1.4	3.8009	10.9	2.5348	-26.0	2.9016	-15.3
	1000	5.04762	5.07189	0.5	6.0731	20.3	4.4730	-11.4	5.1532	2.1
1.0	0.01	0.00994	0.01000	0.6	0.0100	0.6	0.0092	-7.4	0.0087	-12.5
	0.1	0.09507	0.09564	0.6	0.0974	2.5	0.0769	-19.1	0.0920	-3.2
	1.0	0.69023	0.69176	0.2	0.7805	13.1	0.4737	-31.4	0.5890	-14.7
	10	2.59380	2.48454	-4.2	2.8499	9.9	1.6934	-34.7	2.0261	-21.9
	100	4.47530	4.45886	-0.4	5.2159	16.5	3.6329	-18.8	4.2326	-5.4
	1000	5.73011	5.77022	0.7	7.5287	31.4	5.8376	1.9	6.5380	14.1
10	0.01	0.00991	0.00997	0.6	0.0100	0.9	0.0094	-5.1	0.0100	0.9
	0.1	0.09762	0.09802	0.4	0.0983	0.7	0.0829	-15.1	0.0966	-1.0
	1.0	0.84481	0.83817	-0.8	0.8249	-2.4	0.5514	-34.7	0.7463	-11.7
	10	3.23577	3.19191	-1.4	3.1438	-2.8	2.0407	-36.9	2.6194	-19.0
	100	4.81965	4.84167	0.5	5.6481	17.4	4.2583	-11.6	4.8663	1.0
	1000	6.33157	6.37361	0.7	7.9809	26.0	6.5966	4.2	7.1799	13.4

Table 5.4 Comparison of integrated absorptances for NO fundamental band (T = 300°K); $\bar{A}_E$ = LBL = line-by-line results (exact), PD = $[(\bar{A}-\bar{A}_E)/\bar{A}_E] \times 100$, QRB = quasi-random band results.

P (atm)	Opt. Path	Integrated Absorptance, $\bar{A} = A/A_o$ (Nondimensional)								
		LBL	QRB		Tien & Lowder		Cess & Tiwari		Felske & Tien	
	u	$\bar{A}_E$	$\bar{A}$	PB	$\bar{A}$	PB	$\bar{A}$	PB	$\bar{A}$	PB
0.01	0.01	0.00607	0.01306	115.0	0.0068	12.0	0.0045	-26.0	0.0032	-47.0
	0.1	0.02375	0.03955	67.0	0.0180	-24.0	0.0208	-12.4	0.0204	-14.1
	1.0	0.08086	0.13251	64.0	0.0303	-63.0	0.0756	-6.5	0.0706	-12.7
	10	0.28949	0.43065	49.0	0.1181	-59.0	0.2420	-16.4	0.2248	-22.0
	100	0.92456	1.25337	35.0	0.7263	-21.5	0.6930	-25.0	0.6746	-27.0
	1000	2.55159	3.16153	24.0	2.4413	-4.3	1.6805	-34.0	1.7994	-29.0
0.1	0.01	0.00894	0.00977	9.3	0.0093	4.0	0.0068	-24.0	0.0067	-25.0
	0.1	0.06350	0.07755	22.0	0.0578	-9.0	0.0394	-38.0	0.0422	-34.0
	1.0	0.25462	0.34331	35.0	0.1600	-37.0	0.1657	-35.0	0.1639	-36.0
	10	0.86630	1.12599	30.0	0.5737	-34.0	0.5396	-38.0	0.5304	-39.0
	100	2.51921	3.06630	22.0	9.0365	-19.0	1.4088	-44.0	1.4866	-41.0
	1000	5.27990	5.75481	9.0	4.1978	-20.0	2.9078	-45.0	3.3235	-37.0
1.0	0.01	0.00991	0.01001	1.0	0.0099	-0.1	0.0083	-16.0	0.0095	-4.1
	0.1	0.09378	0.09655	3.0	0.0890	-5.1	0.0608	-35.0	0.0719	-23.0
	1.0	0.63506	0.72239	14.0	0.5047	-21.0	0.3121	-51.0	0.3383	-47.0
	10	2.23890	2.63281	18.0	1.6738	-25.0	1.0546	-53.0	1.1378	-49.0
	100	5.04365	5.40347	7.1	3.6985	-27.0	2.4628	-51.0	2.8097	-44.0
	1000	6.79166	7.14657	5.2	5.9678	-12.0	4.3799	-36.0	5.0510	-26.0
10	0.01	0.00991	0.00997	0.6	0.0100	0.9	0.0091	-8.1	0.0099	-0.1
	0.1	0.09792	0.09851	0.6	0.0972	-0.7	0.0763	-22.0	0.0914	-6.6
	1.0	0.87160	0.87741	0.7	0.7725	-11.0	0.4660	-47.0	0.5750	-34.0
	10	3.98050	4.04590	1.6	2.8026	-30.0	1.6608	-58.0	1.9767	-50.0
	100	6.22197	6.41691	3.1	5.1503	-17.0	3.5744	-43.0	4.1673	-33.0
	1000	7.41852	7.64331	3.0	7.4606	0.6	5.7666	-22.0	6.4721	-13.0

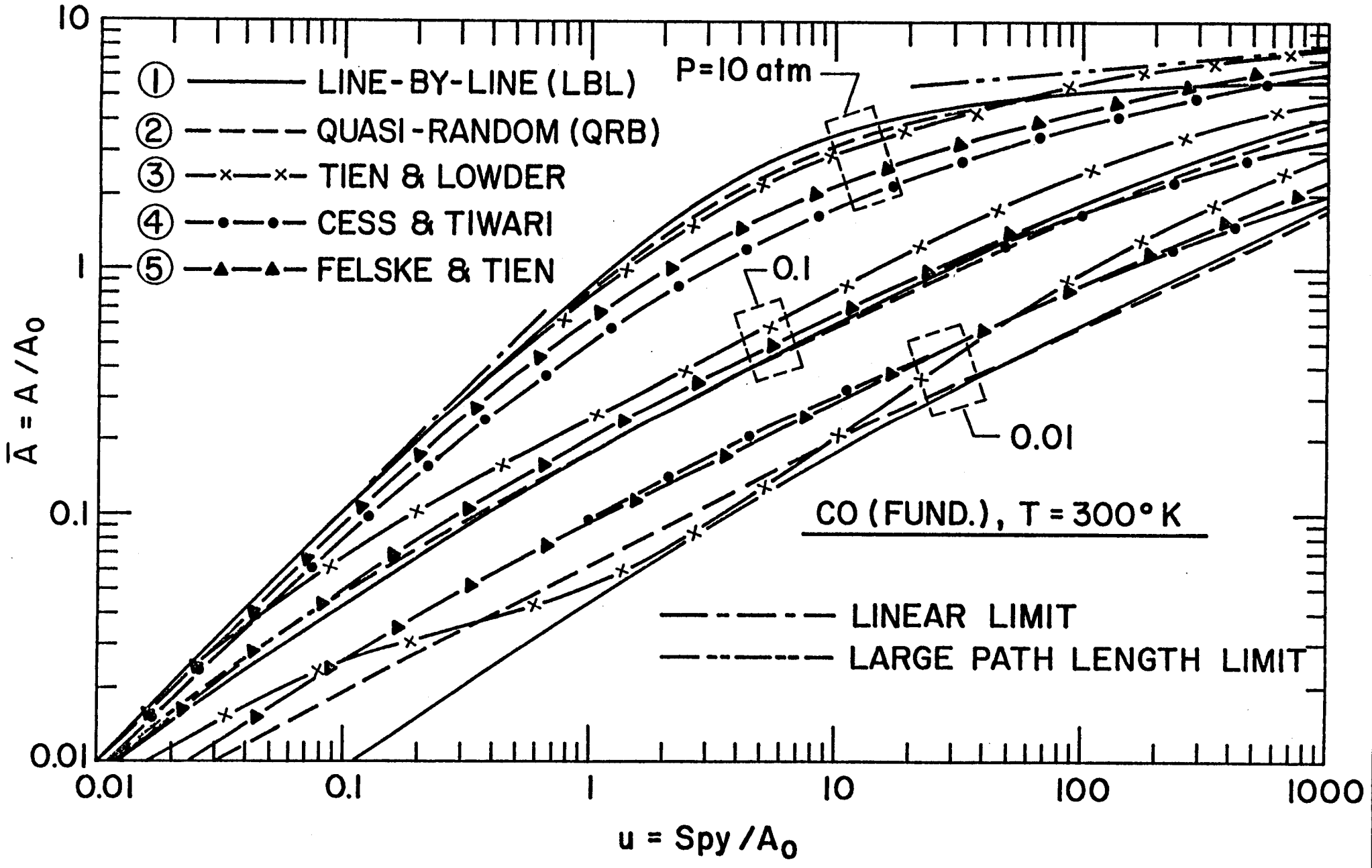

Fig. 5.1a Comparison of band absorptance results for the CO fundamental band at T = 300°K.

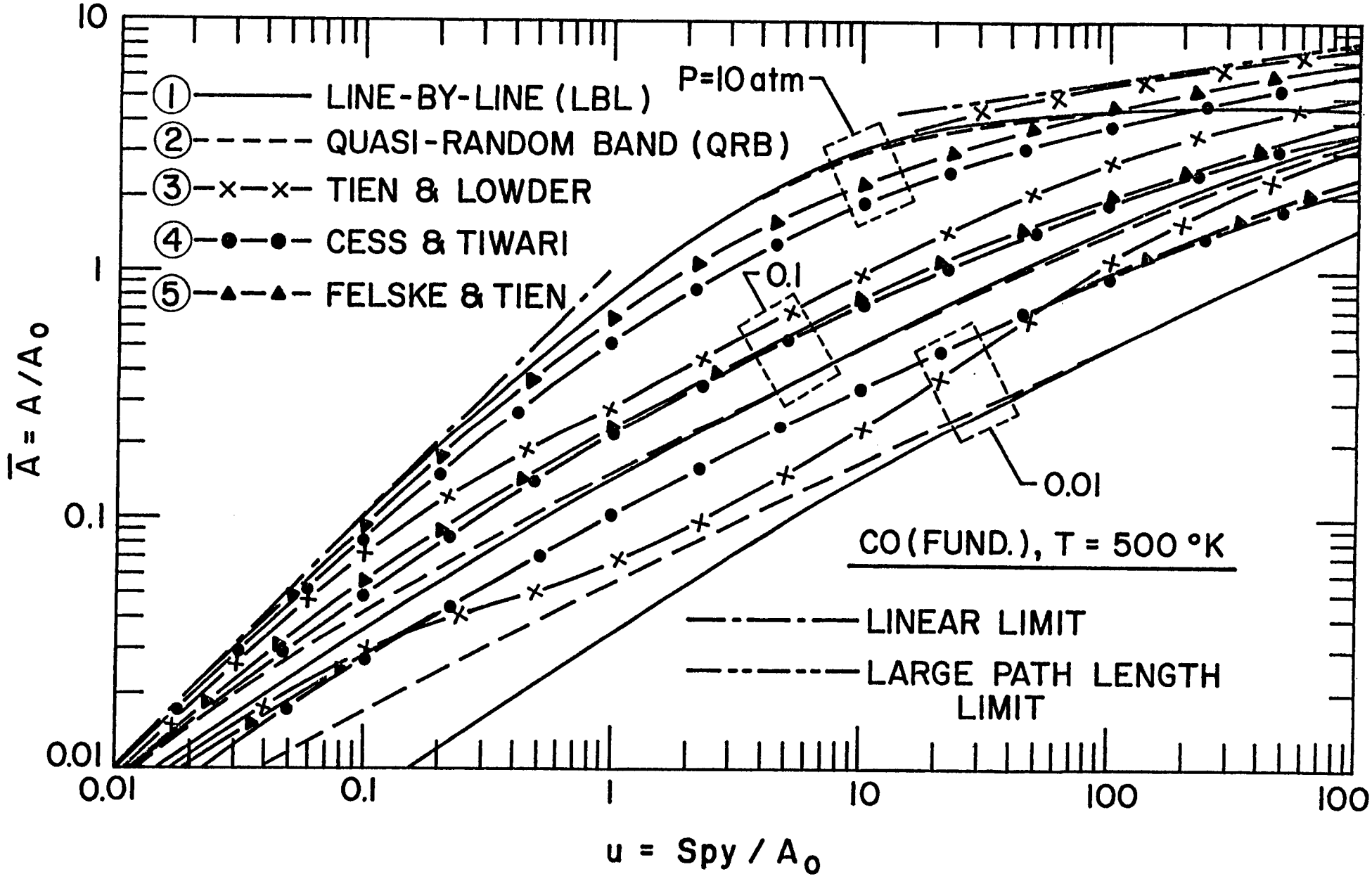

Fig. 5.1b Comparison of band absorptance results for the CO fundamental band at T = 500°K.

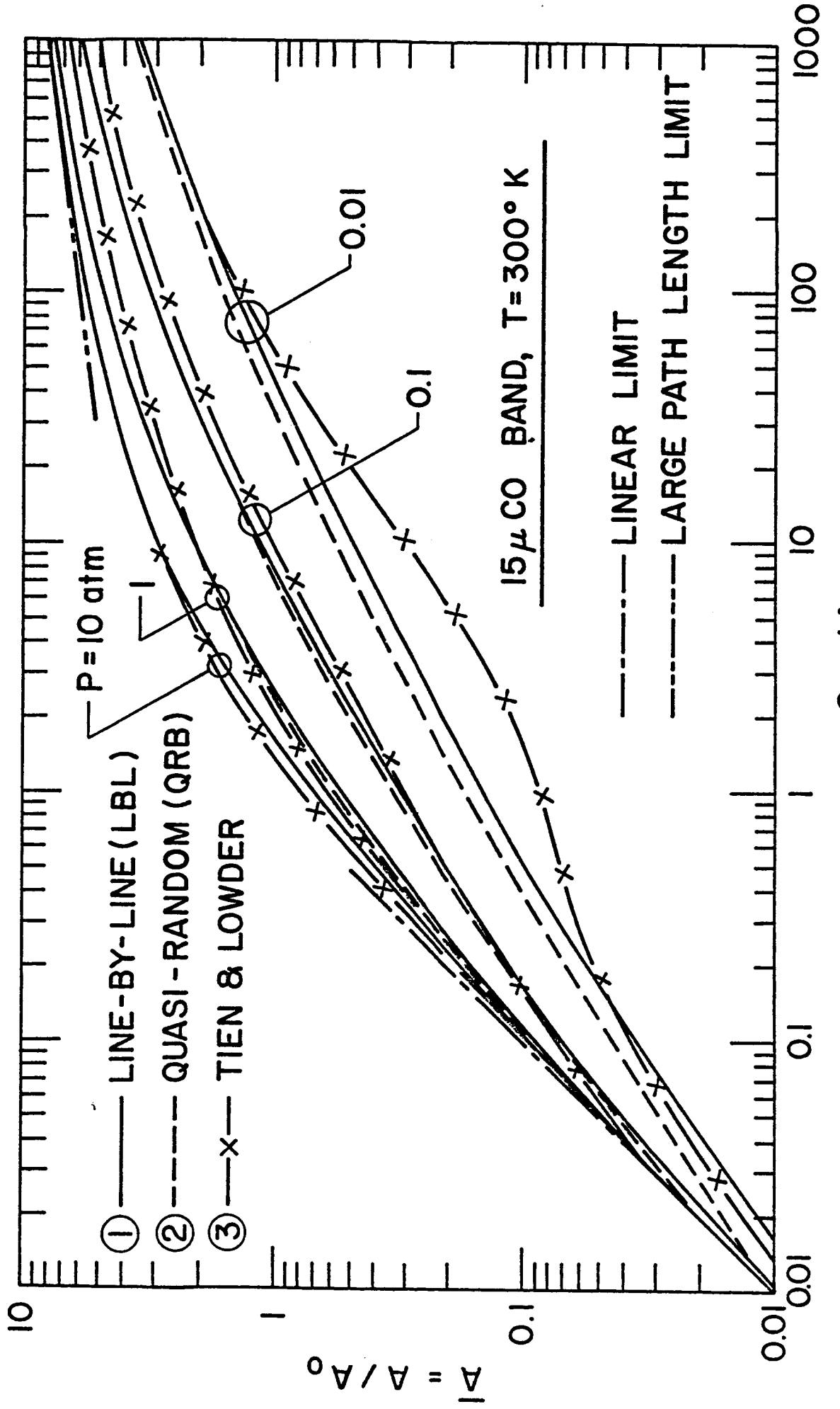

Fig. 5.2a Comparison of band absorptance results for the 15μ CO_2 band at T = 300°K.

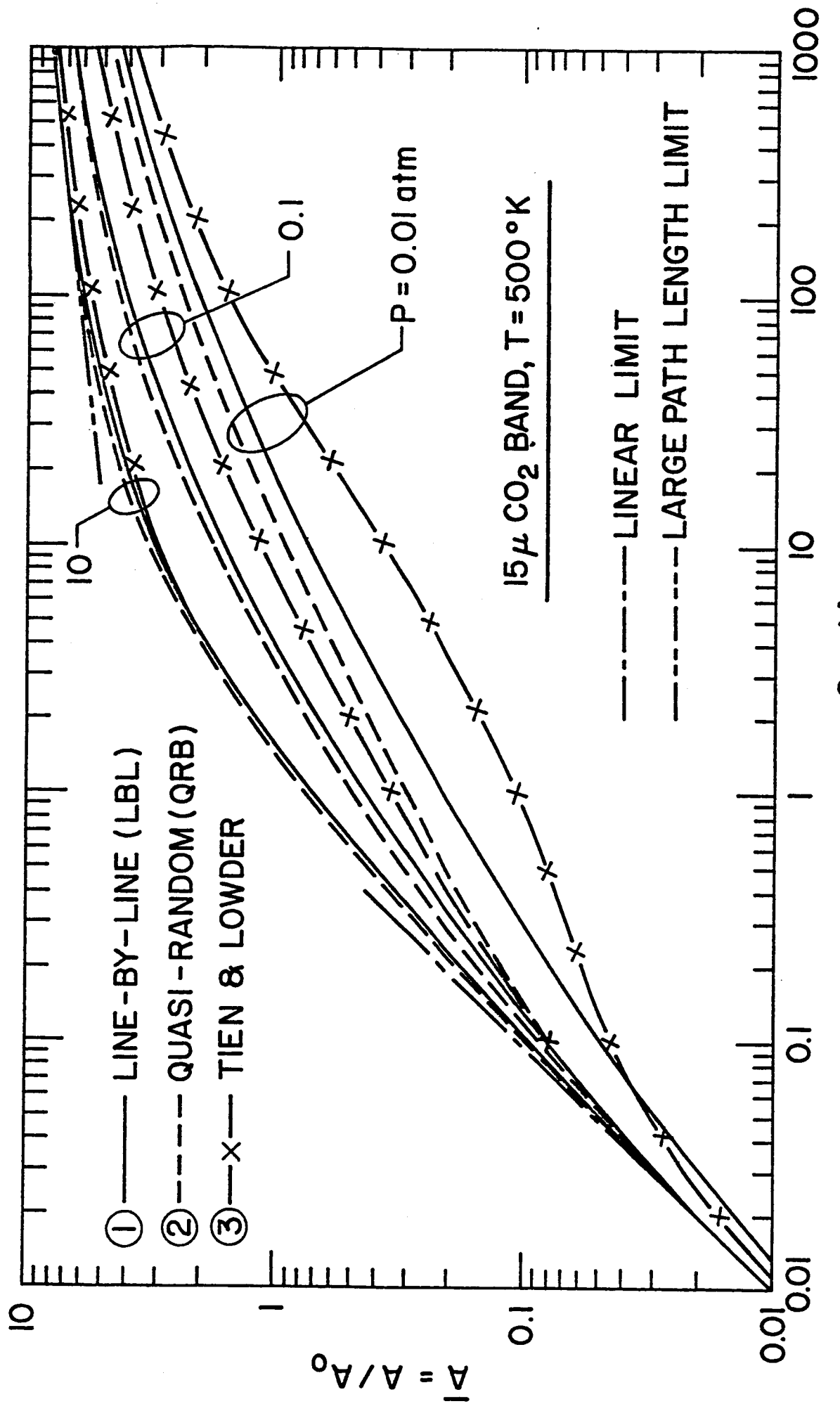

Fig. 5.2b Comparison of band absorptance results for the 15μ CO_2 band at T = 500°K.

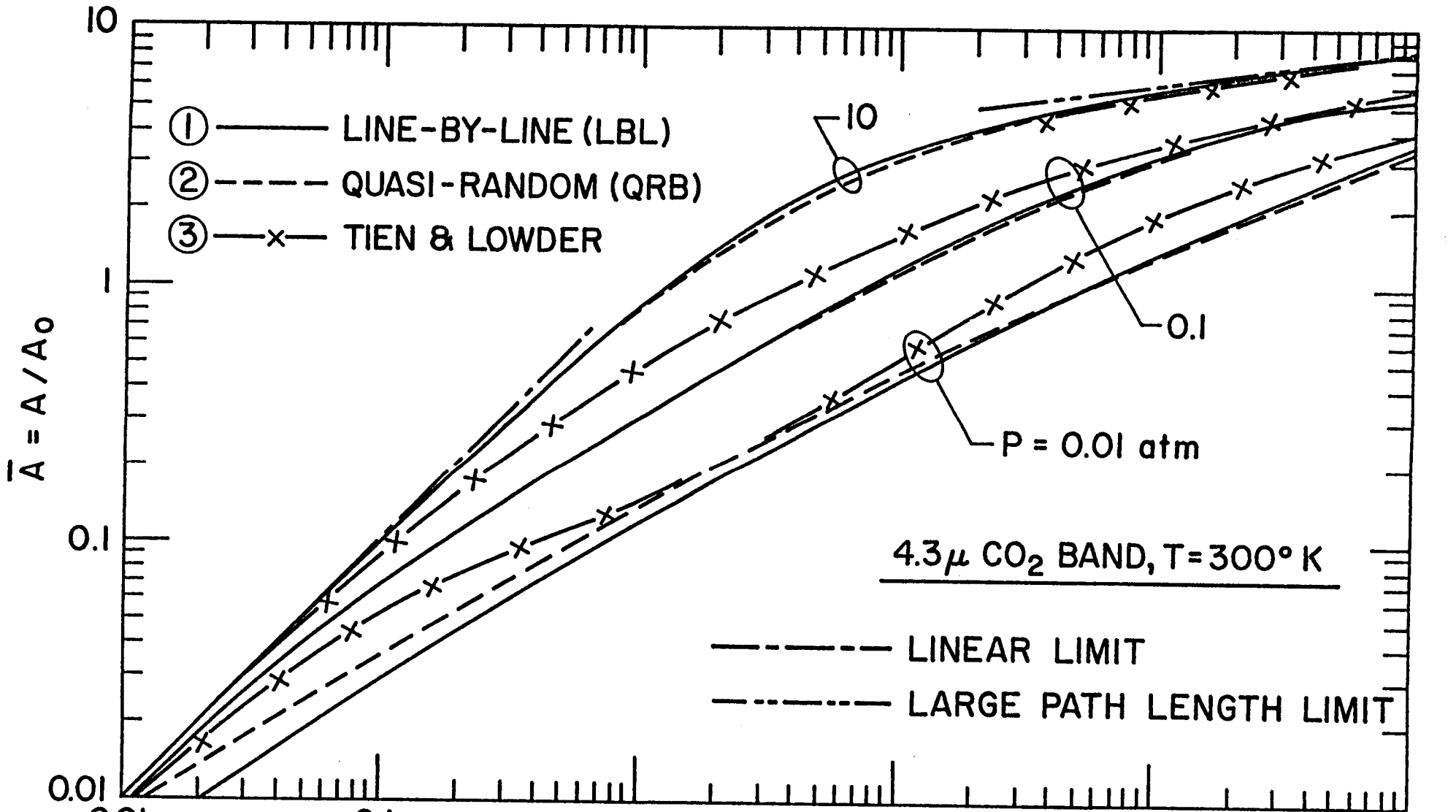

Fig. 5.3a Comparison of band absorptance results for the 4.3μ CO_2 band at T = 300°K.

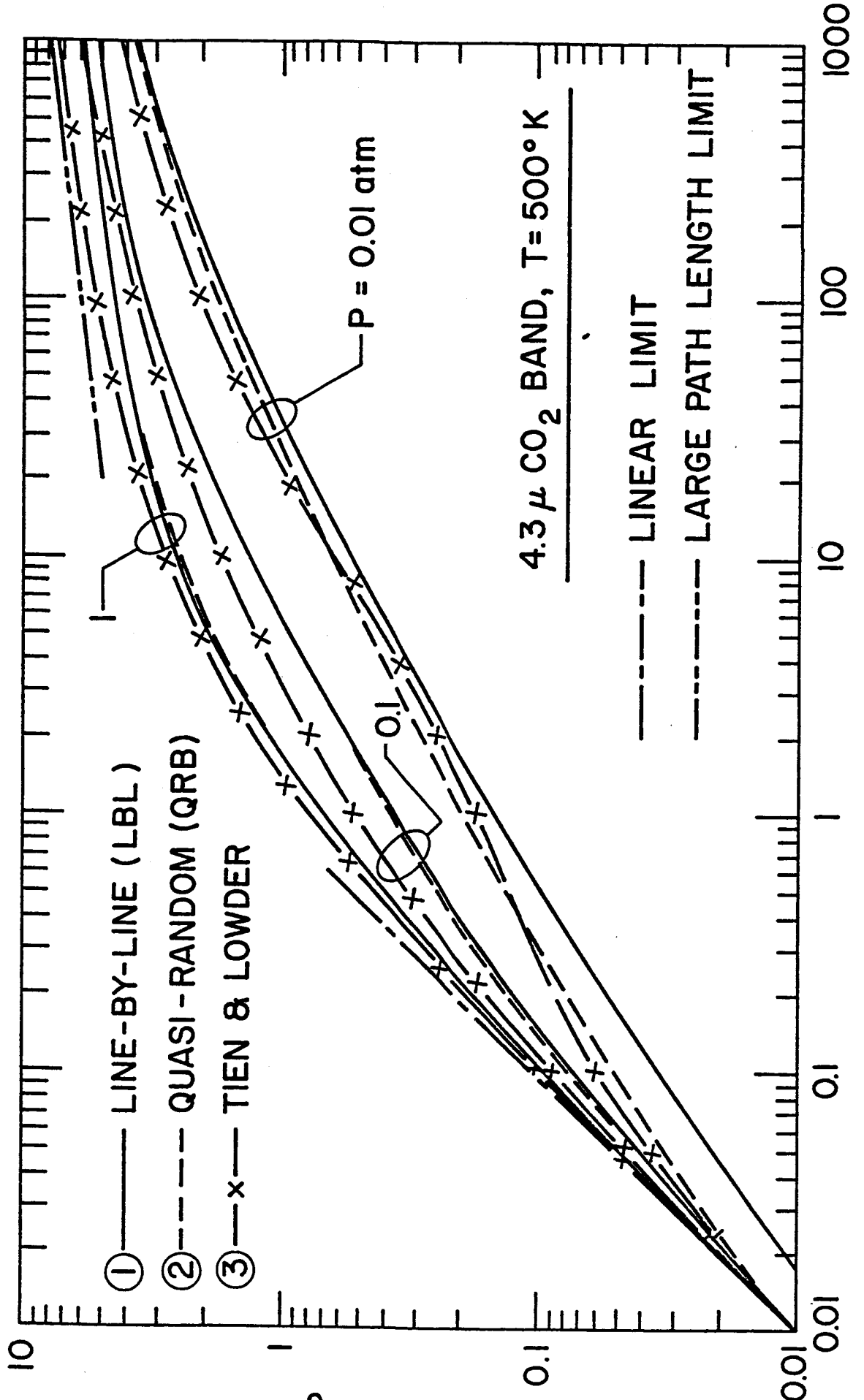

Fig. 5.3b Comparison of band absorptance results for the 4.3μ CO_2 band at T = 500°K.

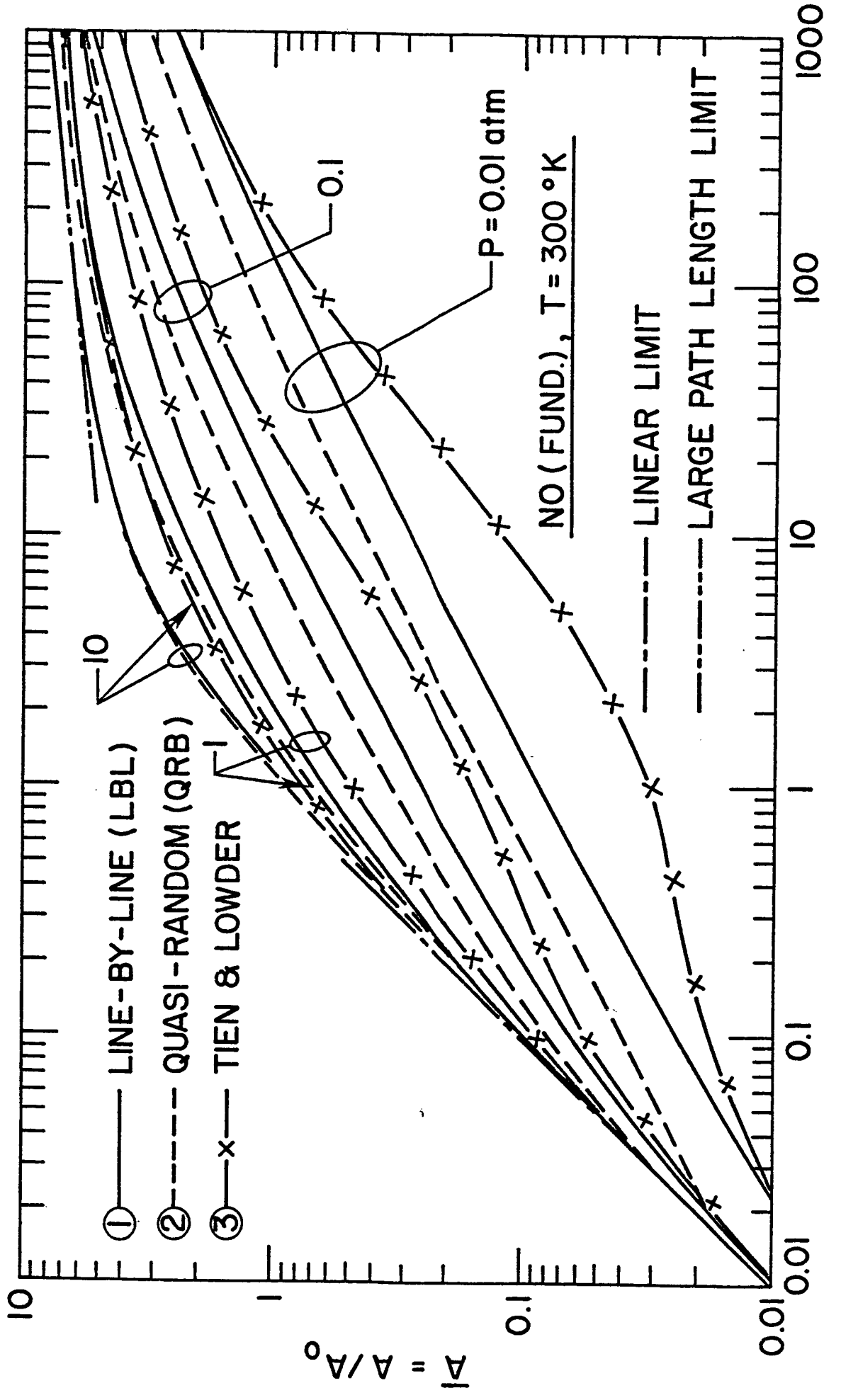

Fig. 5.4 Comparison of band absorptance results for the NO fundamental band at T = 300°K.

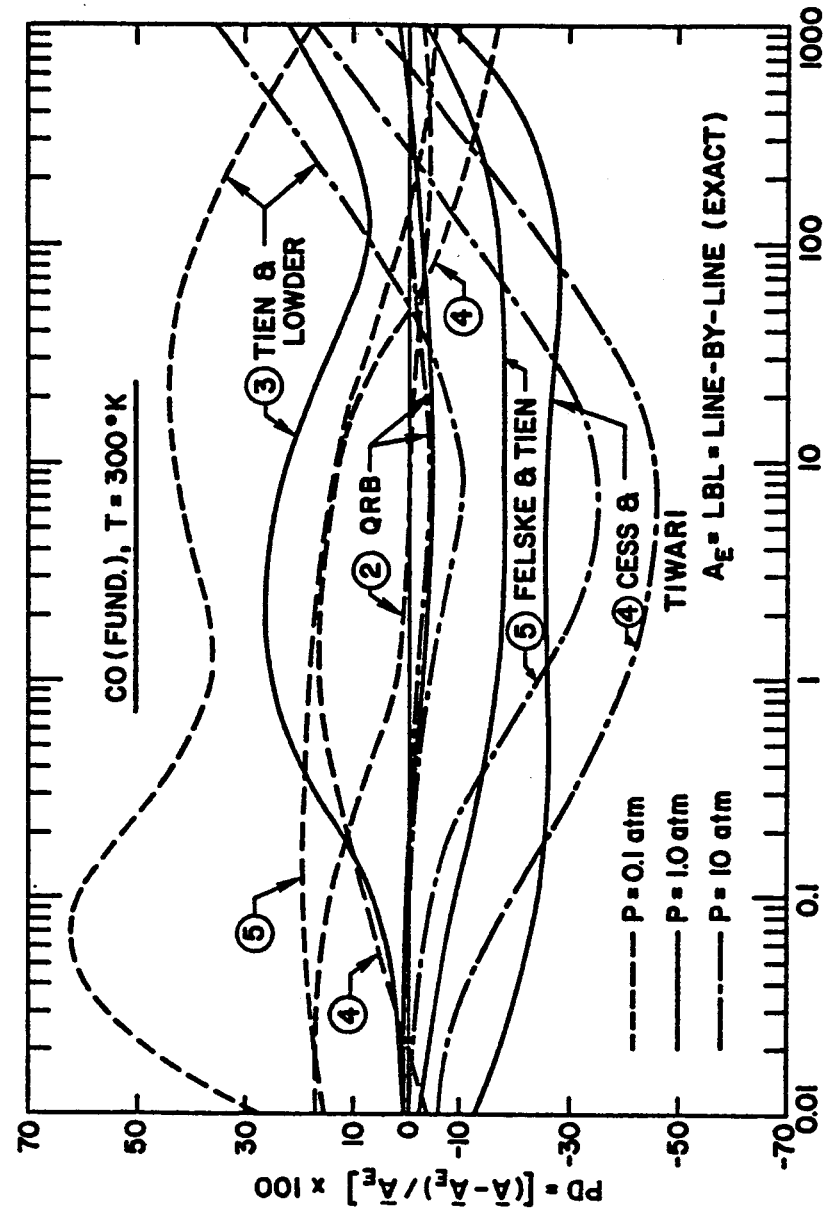

Fig. 5.5 Errors in the total band absorptance by using the various correlations and QRB formulation for the CO fundamental band at T = 300°K.

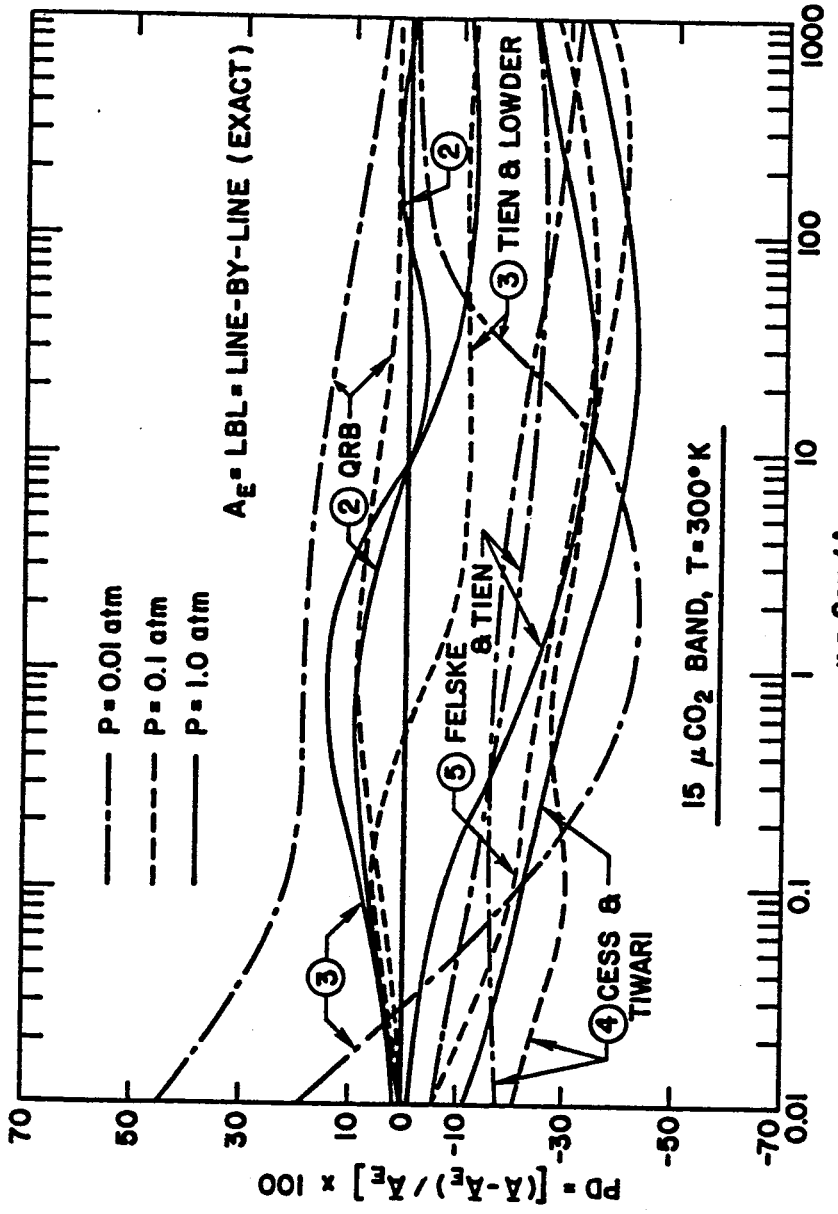

Fig. 5.6 Errors in the total band absorptance by using the various correlations and QRB formulation for the 15μ CO_2 band at T = 300°K.

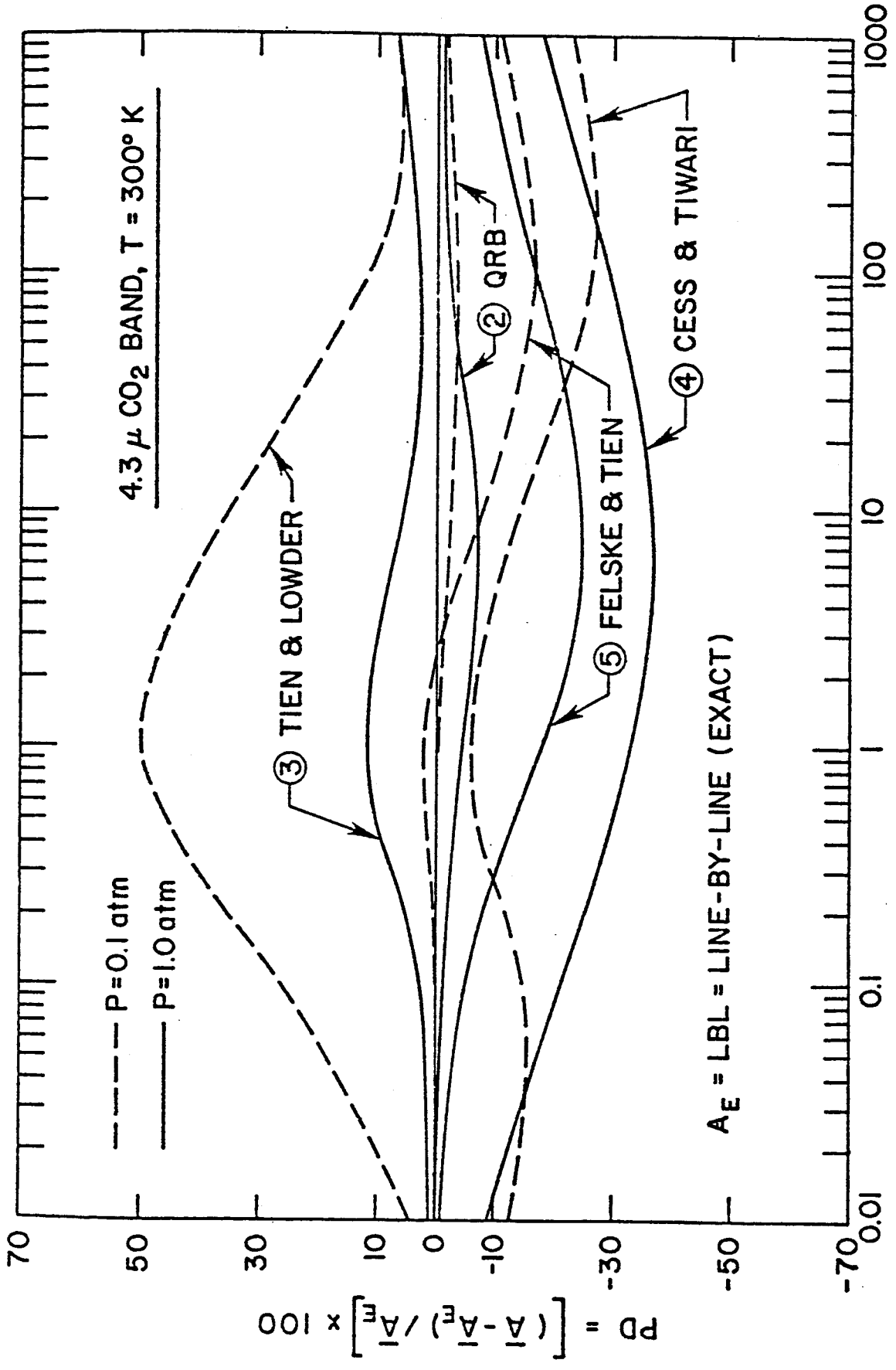

Fig. 5.7 Errors in the total band absorptance by using the various correlations and QRB formulation for the 4.3μ CO_2 band at T = 300°K.

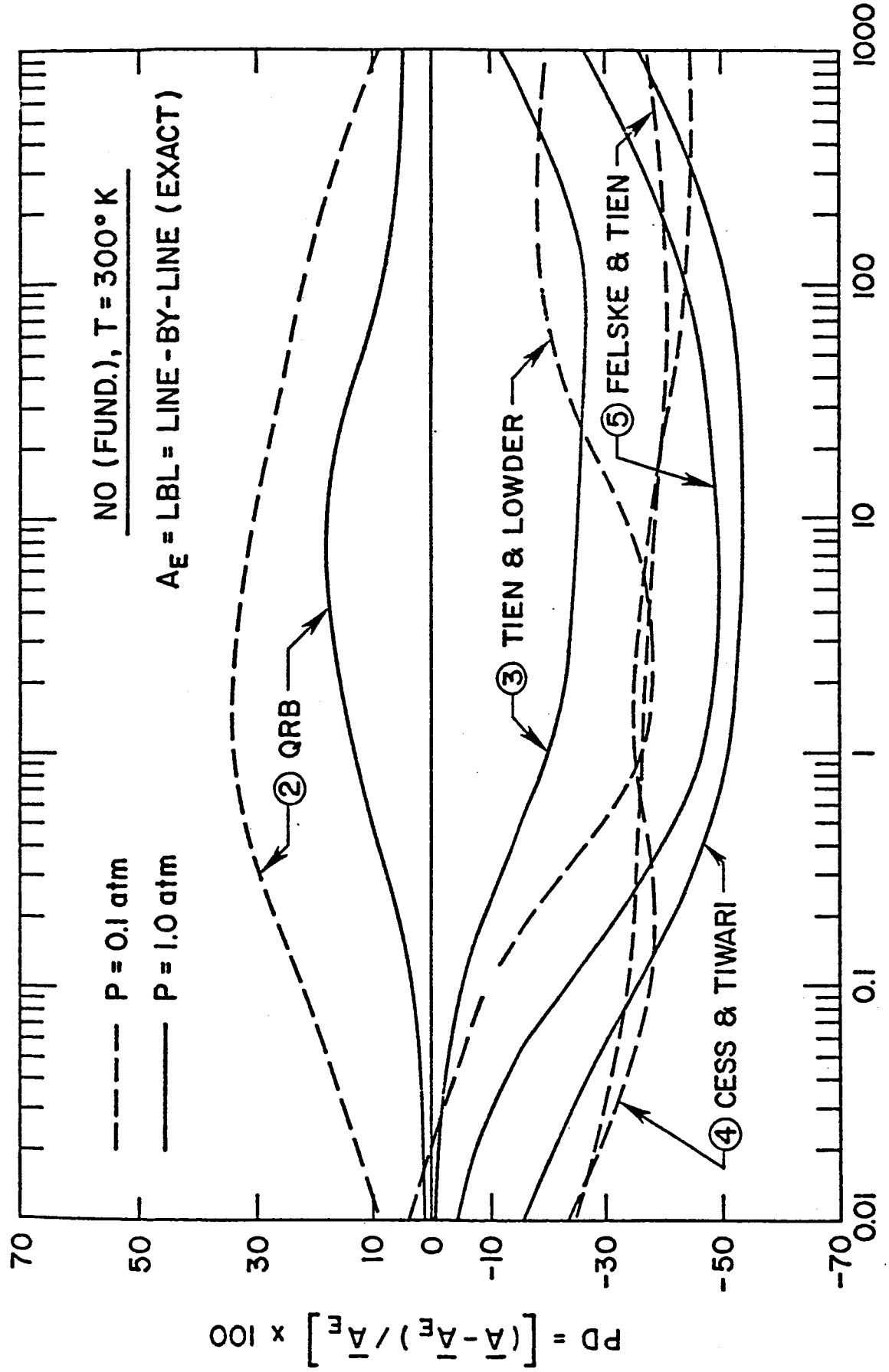

Fig. 5.8 Errors in the total band absorptance by using the various correlations and QRB formulation for the NO fundamental band at T = 300°K.

6. CONCLUSIONS

It has been demonstrated that the line-by-line model is probably the best theoretical approach to calculate the spectral transmittance and total absorptance of a vibration-rotation band. Although it requires a considerably long computational time, the results obtained by this model are in excellent agreement with the available experimental results. The quasi-random band model requires relatively less computational time and yields accurate results in most cases. As such, use of these theoretical models is suggested for radiative transfer analysis requiring high degree of accuracy.

Relative validity of various correlations (Tien and Lowder, Felske and Tien, and Cess and Tiwari), under different pressure and path length conditions, has been established. These correlations require significantly less computational time and yield results with varying degree of accuracy depending upon the nature of the gas. The computer time required by the Felske and Tien correlation is relatively longer than Tien and Lowder, and Cess and Tiwari correlations. Results of specific and general parametric comparisons indicate that use of the Tien and Lowder correlation is justified to all gases under investigation at relatively high pressures. Use of the Felske and Tien, and Cess and Tiwari correlations is recommended for lower and moderate pressures.

REFERENCES

1. Mitchell, A.C.G. and Zemansky, W. M., Resonance Radiation and Excited Atoms, Cambridge Univ. Press., Cambridge, Mass., 1934 (reprinted 1961).

2. Elsasser, W. M., "Heat Transfer by Infrared Radiation in the Atmosphere," Howard Meteorological Studies, No. 6, Harvard Univ. Press, Cambridge, Mass., 1942.

3. Penner, S. S., "Equilibrium Radiation Properties of Gases," Handbook of Heat Transfer, edited by W. M. Rohsenow and J. P. Hartnett, Section 15, Part D, pp. 15-72, McGraw-Hill, New York, 1973.

4. Plass, G. N., "Models for Spectral Band Absorption," Journal of the Optical Society of America, Vol. 48, No. 10, Oct. 1958, pp. 690-703.

5. Plass, G. N., "Useful Representations for Measurements of Spectral Band Absorption," Journal of the Optical Society of America, Vol. 50, No. 9, Sept. 1960, pp. 868-875.

6. Wyatt, P. J., Stull, V. R., and Plass, G. N., "Quasi-Random Model of Band Absorption," Journal of the Optical Society of America, Vol. 52, No. 11, Nov. 1962, pp. 1209-1217.

7. Goody, R. M., Atmospheric Radiation I: Theoretical Basis, Oxford Univ. Press, London and New York, 1964.

8. Edwards, D. K. and Menard, W. A., "Comparison of Methods for Correlation of Total Band Absorption," Applied Optics, Vol. 3, No. 5, May 1964, pp. 621-625.

9. Edwards, D. K., Glassen, L. K., Hauser, W. C., and Tuchscher, J. S., "Radiation Heat Transfer in Nonisothermal Nongray Gases," Journal of Heat Transfer, Vol. 89, Series C, No. 3, Aug. 1967, pp. 219-229.

10. Tien, C. L. and Lowder, J. E., "A Correlation for Total Band Absorptance of Radiating Gases," International Journal of Heat and Mass Transfer, Vol. 9, No. 7, July 1966, pp. 698-701.

11. Tien, C. L., "Thermal Radiation Properties of Gases," Advances in Heat Transfer, Vol. V, Academic Press, New York, 1968.

12. Cess, R. D. and Tiwari, S. N., "Infrared Radiative Energy Transfer in Gases," Advances in Heat Transfer, Vol. VIII, Academic Press, New York, 1972.

13. Edwards, D. K., "Molecular Gas Band Radiation," Advances in Heat Transfer, Vol. XII, Academic Press, New York, 1976.

14. Felske, J. D. and Tien, C. L., "A Theoretical Closed Form Expression for the Total Band Absorptance of Infrared-Radiating Gases," International Journal of Heat and Mass Transfer, Vol. 17, No. 1, Jan. 1974, pp. 155-158.

15. Chan, S. H., "Geometric Band Absorptance for a Nongray Gas with Arbitrary Configurations," International Journal of Heat and Mass Transfer, Vol. 17, 1974, pp. 381-383.

16. Tiwari, S. N., "Band Models and Correlations for Infrared Radiation," AIAA Paper 75-699, 1975. Also published in Progress in Astronautics and Aeronautics (Radiative Transfer and Thermal Control), Vol. 49, 1976, pp. 155-182, AIAA, New York.

17. Tiwari, S. N., "Models for Infrared Atmospheric Radiation," TR-76-T10, June 1976, School of Engineering, Old Dominion University, Norfolk, Va. Also to appear in Advances in Geophysics.

18. Tiwari, S. N., "Application of Infrared Band Model Correlations to Nongray Radiation." Accepted for publication in the International Journal of Heat and Mass Transfer.

19. Gupta, S. K. and Tiwari, S. N., "Evaluation of Upwelling Infrared Radiance from Earth's Atmosphere," TR-75-T14, Nov. 1975. School of Engineering, Old Dominion University, Norfolk, Va.

20. Gupta, S. K. and Tiwari, S. N., "Evaluation of Transmittance of Selected Infrared Bands," TR-76-T7, April 1976, School of Engineering, Old Dominion University, Norfolk, Va.

21. Tiwari, S. N., and Gupta, S. K., "Evaluation of Upwelling Infrared Radiance from the Earth's Troposphere," ASME-AIChE Heat Transfer Conference, Aug. 1976, ASME 76-HT-5.

22. Hsieh, T. C. and Greif, R., "Theoretical Determination of the Absorption Coefficient and the Total Band Absorptance Including a Specific Application to Carbon Monoxide," International Journal of Heat and Mass Transfer, Vol. 15, No. 8, Aug. 1972, pp. 1477-1487.

23. Lin, J. C., and Greif, R., "Theoretical Determination of Absorption with an Emphasis on High Temperatures and a Specific Application to Carbon Monoxide," Journal of Heat Transfer, Trans. ASME, Series C, Vol. 95, 1973, pp. 535-538.

24. Hashemi, A., Hsieh, T. C., and Greif, R., "Theoretical Determination of Band Absorptance with Specific Application to Carbon Monoxide and Nitric Oxide," ASME Paper No. 76-HT-1. To appear in Journal of Heat Transfer.

25. Green, R. M., and Tien, C. L., "Infrared Radiation Properties of Nitric Oxide at Elevated Temperatures," Journal of Quantitative Spectroscopy and Radiative Transfer, Vol. 10, 1970, pp. 805-817.

26. Drayson, S. R., "Atmospheric Transmission in the CO_2 Bands Between 12μ and 18μ," Applied Optics, Vol. 5, No. 3, 1966, pp. 385-392.

27. Kunde, V. G., "Theoretical Computations of the Outgoing Infrared Radiance from a Planetary Atmosphere," TR D-4045, Aug. 1967, NASA.

28. Kunde, V. G. and Maguire, W. C., "Direct Integration Transmittance Model," Journal of Quantitative Spectroscopy and Radiative Transfer, Vol. 14, No. 8, Aug. 1974, pp. 803-817.

29. McClatchey, R. A., Benedict, W. S., Clough, S. A., Burch, D. E., Calfee, R. F, Fox, K., Rothman, L.S., and Garing, J. S., "AFCRL Atmospheric Line Parameters Compilation," AFCRL-TR-73-0096, Jan. 1973, Air Force Cambridge Research Laboratories, Bedford, Mass.

30. Burch, E. E., Gryvnak, D. A., Singleton, E. B., France, W. L., and Williams, D., "Infrared Absorption by Carbon Dioxide, Water Vapor, and Minor Atmospheric Constituents," AFCRL-62-698, July 1962, Air Force Cambridge Research Laboratories, Bedford, Mass.

31. Abu-Romia, M. M., and Tien, C. L., "Measurements and Correlations of Infrared Radiation of Carbon Monoxide at Elevated Temperatures," Journal of Quantitative Spectroscopy and Radiative Transfer, Vol. 6, 1966, pp. 143-167-

32. Young, C., "A Study of the Influence of Carbon Dioxide on Radiative Transfer in the Stratosphere and Mesosphere," Technical Report, March 1964, Dept. of Meteorology and Oceanography, College of Engineering, University of Michigan, Ann Arbor, Mich.

33. Goldman, A., and Schmidt, S. C., "Infrared Spectral Line Parameters and Absorptance Calculations of NO at Atmospheric and Elevated Temperatures for the $\Delta u = 1$ Bands Regions," Journal of Quantitative Spectroscopy and Radiative Transfer, Vol. 15, 1975, pp. 127-138.